

UNCLASSIFIED

AD NUMBER

AD821909

LIMITATION CHANGES

TO:

Approved for public release; distribution is unlimited.

FROM:

Distribution authorized to U.S. Gov't. agencies and their contractors;  
Administrative/Operational Use; 18 SEP 1967.  
Other requests shall be referred to Air Force Technical Applications Center, Washington, DC 20330.

AUTHORITY

AFTAC ltr 25 Jan 1972

THIS PAGE IS UNCLASSIFIED

AD821909



TEXAS INSTRUMENTS  
INCORPORATED



VELA T/7701

## ADAPTIVE FILTERING OF SEISMIC ARRAY DATA

### ADVANCED ARRAY RESEARCH

Special Report No. 1

Prepared by

John P. Burg   Aaron H. Booker   Ronald J. Holyer

George D. Hair Jr., Program Manager  
1-214-238-3473

TEXAS INSTRUMENTS INCORPORATED

Science Services Division

P.O. Box 5621

Dallas, Texas 75222

Contract: F33657-67-C-0708-P001

Contract Date: 15 December 1966

Amount of Contract: \$625,500

Contract Expiration Date: 14 December 1967

Sponsored by

ADVANCED RESEARCH PROJECTS AGENCY

Nuclear Test Detection Office

ARPA Order No. 624

ARPA Program Code No. 7F10

18 September 1967



## ACKNOWLEDGMENT

This research was supported by the  
ADVANCED RESEARCH PROJECTS AGENCY  
Nuclear Test Detection Office  
under Project VELA UNIFORM  
and accomplished under the technical direction of the  
AIR FORCE TECHNICAL APPLICATIONS CENTER  
under Contract No. F33657-67-C-0708-P001



---

## ABSTRACT

Adaptive multichannel prediction filtering has been completed on four data samples, and adaptive maximum-likelihood signal extraction has been done on one sample.

Comparison of adaptive results with those obtained from processing the same data with stationary filters (nonchanging filters designed from correlation-function estimates) shows that the adaptive filters approach the stationary filters as  $k_g$  (the rate-of-convergence parameter in the adaptive algorithm) approaches 0. For larger values of  $k_g$ , adaptive prediction-error filtering does better than stationary filters on nontime-stationary data, but stationary filters are better on data samples which appear to be time-uniform.

The performance of an adaptively designed maximum-likelihood filter was shown to be essentially equivalent to that of a maximum-likelihood filter which was conventionally designed from correlation-function estimates.



## TABLE OF CONTENTS

Section	Title	Page
	ABSTRACT	iii/iv
I	INTRODUCTION AND SUMMARY	I-1/2
II	THEORY OF ADAPTIVE FILTERING	II-1
	A. SINGLE-CHANNEL PREDICTION	II-1
	B. MULTICHANNEL PREDICTION FILTERING	II-3
	C. MAXIMUM-LIKELIHOOD SIGNAL EXTRACTION	II-5
III	EXPERIMENTAL RESULTS	III-1
	A. PREDICTION FILTERING	III-1
	1. UBO Road Noise	III-1
	2. UBO Normal Noise	III-7
	3. LASA Subarray B1	III-15
	4. Array Data	III-21
	B. MAXIMUM-LIKELIHOOD FILTERING	III-21
IV	CONCLUSIONS AND RECOMMENDATIONS	IV-1
V	REFERENCES	V-1/2

## TABLE

Table	Title	Page
III-1	Summary of Data Processed	III-2



## LIST OF ILLUSTRATIONS

Figure	Description	Page
II-1	Block Diagram of Multichannel Prediction Scheme	II-4
III-1	Prefiltered and Resampled UBO Road Noise and UBO Array Geometry	III-3
III-2	UBO Road Noise, Mean-Square-Error Vs $k_s$	III-5
III-3	UBO Road Noise, Mean-Square-Error Vs Time	III-6
III-4	UBO Road Noise, Power Spectra of Channel 10, and Adaptive Errors	III-8
III-5	UBO Road Noise, Wiener and Adaptive Filter Outputs	III-9
III-6	Prefiltered and Resampled UBO Normal Noise	III-10
III-7	UBO Normal Noise, Mean-Square-Error Vs $k_s$	III-11
III-8	Normal Noise, Mean-Square-Error Vs Time	III-13
III-9	UBO Normal Noise, Wiener and Adaptive Filter Outputs	III-14
III-10	LASA Subarray B1 Center Seismometer and First Ring Prefiltered and Resampled	III-16
III-11	LASA Subarray B1 Center Seismometer and First Ring, Mean-Square-Error Vs $k_s$	III-17
III-12	LASA Subarray B1 Center Seismometer and First Ring, Mean-Square-Error Vs Time	III-18
III-13	LASA Subarray B1 Center Seismometer and First Ring — Power Spectra of Channel 1, Wiener Error, and Adaptive Errors	III-19
III-14	LASA Subarray B1 Center Seismometer and First Ring, Wiener and Adaptive Filter Outputs	III-20
III-15	Prefiltered and Resampled Array Data	III-22
III-16	Array Data, Mean-Square-Error Vs $k_s$	III-23
III-17	Array Data, Mean-Square-Error Vs Time	III-24
III-18	Array Data, Wiener and Adaptive Filter Outputs	III-25
III-19	Maximum-Likelihood Filter Outputs	III-27/28



---

## SECTION I

### INTRODUCTION AND SUMMARY

This report presents initial results in a study of the adaptive filtering of seismic array data. There is a brief discussion of the theoretical basis of the adaptive algorithm and its application to multichannel prediction and maximum-likelihood filtering. Adaptive multichannel prediction filtering has been completed on four data samples, and maximum-likelihood signal extraction has been done on one sample. Adaptive filter results are compared with those obtained from stationary filters, i. e., from nonchanging filters designed from correlation function estimates.

Plots of both mean-square-error vs  $k_s$  (the rate-of-convergence parameter in the adaptive algorithm) and of mean-square-error vs time indicate that, in the limit as  $k_s$  approaches 0, the adaptive filters approach the stationary Wiener filters. For larger values of  $k_s$ , the mean-square-error of the adaptive prediction is found to be greater than the Wiener mean-square-error for some data samples and less for other samples. The data characteristic which defines the exact behavior of the mean-square-error-vs- $k_s$  curve appears to be related to the time-stationarity of the data.

The performance of an adaptively designed maximum-likelihood filter was shown to be essentially equivalent to that of a maximum-likelihood filter which was conventionally designed from correlation-function estimates.





## SECTION II

### THEORY OF ADAPTIVE FILTERING

To derive the Widrow adaptive-filter algorithm without becoming too involved with notation, the simple problem of single-channel prediction will be used to illustrate the main features of the algorithm. Later, the algorithm will be expanded to the multichannel case; and its application to maximum-likelihood signal extraction will be discussed.

#### A. SINGLE-CHANNEL PREDICTION

Consider a single channel of sampled data points,  $x_i$ ; and let the problem be to take  $p$  consecutive values of  $x_i$  and use them to predict the value of the next point. To do this, these values of  $x_i$  are considered to be components of a  $p$ -dimensional column vector,

$$\underline{X}_n = (x_{n-p+1}, x_{n-p+2}, x_{n-p+3}, \dots, x_n)^T \quad (2-1)$$

To predict the value of the next point,  $x_{n+1}$ , the scalar product is formed from the data vector  $\underline{X}_n$  with the prediction-filter vector,

$$\underline{F} = (f_1, f_2, f_3, \dots, f_p)^T \quad (2-2)$$

The error in the prediction of  $x_{n+1}$  is

$$e_{n+1} = x_{n+1} - \underline{F}^T \underline{X}_n \quad (2-3)$$



and the squared error is

$$\epsilon_{n+1}^2 = \underline{F}^T \underline{X}_n \underline{X}_n^T \underline{F} - 2 \underline{F}^T \underline{X}_n x_{n+1} + x_{n+1}^2 \quad (2-4)$$

The expected value of  $\epsilon_{n+1}^2$  is given by

$$\overline{\epsilon_{n+1}^2} = \underline{F}^T \overline{\underline{X}_n \underline{X}_n^T} \underline{F} - 2 \underline{F}^T \overline{\underline{X}_n} x_{n+1} + \overline{x_{n+1}^2} \quad (2-5)$$

Equation (2-5) shows the expected value of  $\epsilon_{n+1}^2$  to be representable as a  $n$ -dimensional quadratic surface in  $F$ . The value of  $F$  at which the minimum of the expected  $\epsilon_{n+1}^2$  surface occurs is the optimum filter in the least-squares sense. Adaptive processing starts with some arbitrary filter vector  $F$  and iteratively converges toward the optimum  $F$ . In this report, the  $(n+1)^{th}$  iteration of  $F$ ,  $F_{n+1}$  is found from  $F_n$  by the method of steepest descent, which can be summarized in the following two rules:

- 1) Move opposite the direction of the gradient of the  $\overline{\epsilon_{n+1}^2}$  surface
- 2) The distance moved in this direction is proportional to the magnitude of the gradient, and the constant of proportionality is called  $k_s$

Cast into equation form, these two rules yield the steepest-descent algorithm

$$\underline{F}_{n+1} = \underline{F}_n - k_s \nabla \overline{\epsilon_{n+1}^2} \quad (2-6)$$



In practice, the gradient of the expected value of  $\epsilon_{n+1}^2$  is not known. However, the Widrow adaptive-filter algorithm meets this problem by making the approximation

$$\nabla \overline{\epsilon_{n+1}^2} \approx \nabla \epsilon_{n+1}^2$$

$\nabla \epsilon_{n+1}^2$  is obtained by differentiating Equation (2-4) with respect to  $\underline{F}^T$ , giving

$$\nabla \epsilon_{n+1}^2 = 2 \underline{X}_n \underline{X}_n^T \underline{F}_n - 2 \underline{X}_n x_{n+1} = -2 \epsilon_{n+1} \underline{X}_n \quad (2-7)$$

Combining Equations (2-7) and (2-6) gives the Widrow single channel adaptive algorithm of

$$\underline{F}_{n+1} = \underline{F}_n + 2k_s \epsilon_{n+1} \underline{X}_n \quad (2-8)$$

## B. MULTICHANNEL PREDICTION FILTERING

The multichannel case is shown diagrammatically in Figure II-1. Here, C channels of time-series data are filtered by C digital filters to produce an output which is supposed to approximate  $y_n$ , the desired output. In this diagram, the subscript n used on the filter-column vectors, the input time-series data vectors, the desired output, and the prediction error indicates their values at the  $n^{\text{th}}$  time. The subscript is necessary on the filter vector since the filter weights change with time in the adaptive algorithm.

The derivation of the multichannel algorithm follows easily from the single-channel algorithm if a new column vector  $\underline{X}'_n$  is made by placing the column vectors  $\underline{X}_n(i)$ ,  $i=1$  to C, on top of each other and likewise forming a new column vector  $\underline{F}'_n$  from the  $\underline{F}_n(i)$ ,  $i=1$  to C.

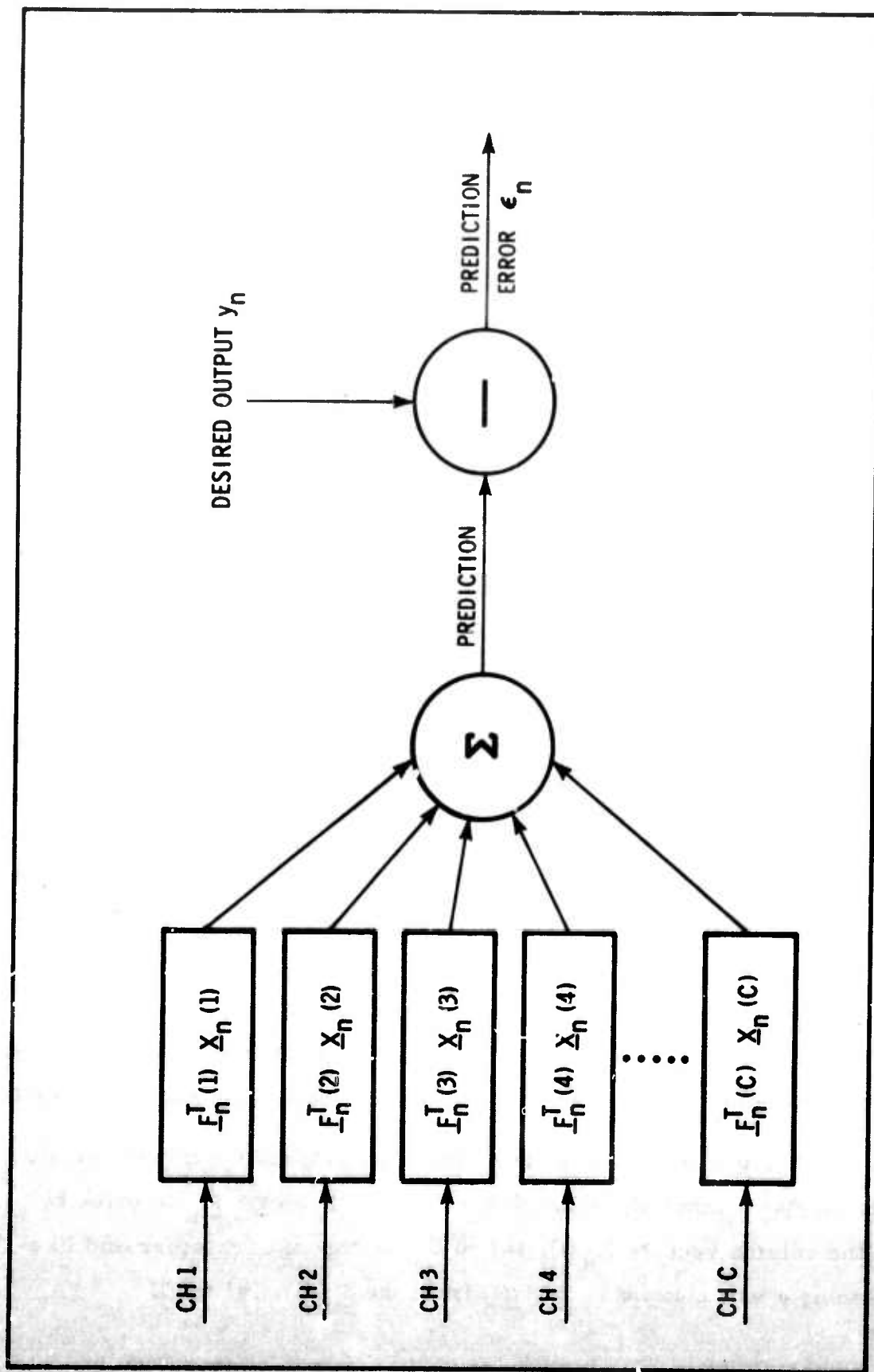


Figure II-1. Block Diagram of Multichannel Prediction Scheme



In terms of the new vectors, the prediction is given by a scalar product of  $\underline{X}'_n$  and  $\underline{F}'_n$ . Thus the prediction error can be written as

$$\epsilon_n = y_n - \underline{F}'_n{}^T \underline{X}'_n \quad (2-9)$$

Using the same general procedure as used in deriving the single-channel algorithm, the multichannel adaptive-filter algorithm is then found to be

$$\underline{F}'_{n+1} = \underline{F}'_n + 2k_s \epsilon_n \underline{X}'_n \quad (2-10)$$

### C. MAXIMUM-LIKELIHOOD SIGNAL EXTRACTION

The transformation of maximum-likelihood processing into problems of prediction is first considered. This transformation is desirable so that the adaptive-prediction method previously described can be used to design maximum-likelihood filters.

Suppose we have an N-channel problem and an L-point filter  $f_{ij}$ , where  $i=1, \dots, N$  and  $j=1, \dots, L$ . We wish to minimize the output of the filter

$$y_{t-s} = \sum_{ij} f_{ij} x_{i,t-j} \quad (2-11)$$

where  $x_{i,t}$  is the output of seismometer  $i$  at time  $t$ . The criterion that  $y_{t-s}$  be an unbiased estimate at time  $t-s$  of the signal, which is assumed constant across channels, leads to the constraints

$$\sum_i f_{ij} = \delta_{js} \quad (2-12)$$



where

$$\delta_{js} = 0 \text{ for } j \neq s$$

and

$$\delta_{js} = 1 \text{ for } j = s$$

The constraints may be expressed as

$$f_{1j} = \delta_{js} - \sum_{i=2}^N f_{ij}$$

and substituted into Equation (2-11). This gives

$$y_{t-s} = \sum_j \left( \delta_{js} - \sum_{i=2}^N f_{ij} \right) x_{1,t-j} + \sum_{i=2}^N \sum_j f_{ij} x_{i,t-j}$$

which can be simplified to the form

$$y_{t-s} = x_{1,t-s} - \sum_{i=2}^N \sum_j f_{ij} (x_{1,t-j} - x_{i,t-j}) \quad (2-13)$$

Referring to Equation (2-3), Equation (2-13) can be recognized as a prediction-error equation. Thus, the maximum-likelihood output  $y_{t-s}$  can be considered the error in predicting  $x_{1,t-s}$  by filters operating on the set of data  $(x_{1,t-j} - x_{i,t-j})$ , where the filters are no longer subject to constraints.

Equations could now be written to specify the filters  $f_{ij}$  in terms of the covariances of the data  $x_{i,t}$ . These equations would be equivalent to the conventional system of equations but of order  $(N-1)L$  instead of  $NL$ . However, the purpose of this section is to determine adaptively the maximum-likelihood filters.



Referring to the algorithm of Equation (2-8) which resulted from Equation (2-3), an adaptive algorithm follows immediately from Equation (2-13). The resulting maximum-likelihood adaptive algorithm is

$$f_{ij}(t+1) = f_{ij}(t) + 2k_s y_{t-s} (x_{1,t-j} - x_{i,t-j}) \quad (2-14)$$

The adaptive maximum-likelihood results in this report are derived by using Equation (2-14). Obviously, there are other ways of combining Equation (2-11) and the constraints of Equation (2-12) into a single prediction-error equation. For example, one could solve for  $f_{3j}$  and substitute into Equation (2-11), thereby predicting channel 3 from traces made by subtracting the remaining channels from channel 3. All of these different ways of producing a prediction-error equation are equivalent in the sense that the resulting equations specifying the filters in terms of the covariances of the data  $x_{i,t}$  define equivalent filters. The adaptive algorithms resulting from the different prediction-error equations will be different, however.

All of these algorithms are determined by reducing the dimension of the problem by substituting in the constraint equation and then by finding the gradient for the reduced set of filter coefficients. The constraints are satisfied by actually using the projection of the subset gradient on the constraint plane. A better method is obtained by finding the gradient at a point in time for the complete set of coefficients and projecting this gradient on the constraint plane. This "full" gradient algorithm can be derived from Equations (2-11) and (2-12) by adding and subtracting

$$\sum_{ij} f_{ij} \bar{x}_{t-j}$$



where

$$\bar{x}_{t-j} = \frac{1}{N} \sum_{i=1}^N x_{i,t-j}$$

Thus,

$$y_{t-s} = \bar{x}_{t-s} - \sum_{ij} f_{ij} (\bar{x}_{t-j} - x_{i,t-j}) \quad (2-15)$$

which is in the form of a prediction-error equation so that the corresponding adaptive algorithm is

$$f_{ij}(t+1) = f_{ij}(t) + 2k_s y_{t-s} (\bar{x}_{t-j} - x_{i,t-j}) \quad (2-16)$$

Note that the constraints are always satisfied if the iteration is started with filters satisfying the constraints.

The final report will give a more complete description of maximum-likelihood processing by the adaptive method of Equation (2-16).





## SECTION III

### EXPERIMENTAL RESULTS

#### A. PREDICTION FILTERING

Adaptive multichannel prediction filtering has been completed on four data samples. Information about these data — which consist of UBO road noise, UBO normal noise, the center and first ring of LASA subarray B1, and 13 channels of array data — is given in Table III-1. These data samples also have been processed using Wiener prediction filters.

In the filtering program, the data in each trace are scaled by  $1/(\text{rms value of that trace})$  so that the variance of all data traces is 1. Thus, results of processing on the different data samples may be compared directly.

Results for each data sample are presented in the form of three figures. The first figure shows mean-square-error vs  $k_g$  and the Wiener filter mean-square-error. The second shows mean-square-error vs time for the Wiener filter, the adaptive filter with the large  $k_g$ , and the adaptive filter with the small  $k_g$ . It should be noted that the origin in these figures does not correspond to zero mean-square-error. The third figure is a plot of the channel to be predicted plus the prediction and prediction error of the Wiener and large and small  $k_g$  filters.

Power spectra of the channel being predicted and of the Wiener and adaptive error traces have been computed for UBO road noise and LASA subarray B1.

##### 1. UBO Road Noise

A major highway passes within a few miles of the northwest extent of the UBO array. The UBO road noise (Figure III-1), which is predominantly Rayleigh energy believed to originate along this highway, does not arrive as a plane wavefront, is time varying, and is attenuated across the array.



Table III-1

## SUMMARY OF DATA PROCESSED

Sample	Date	Time	Data Length		Number of Channels	Channels Used for Prediction	Channel Predicted	Filter Length	Number of Points Ahead Predicted
			After Resampling (points)	(sec)					
UBO road noise	9-23-64	16:06:20	1250	90	10	1 - 9	10	27	-13
UBO normal noise	9-30-64	21:51:10	1250	90	10	1 - 9	10	27	-13
LASA subarray B1 Center and first ring	3-25-66	04:26:43	2200	220	7	1 - 7	1	25	1
Array data	11-20-66	23:14:00	3250	234	13	2 - 13	1	37	-18
LASA subarray C1 First ring omitted (Maximum likelihood processing described in B)	11-10-65	03:48:28	3250	325	19	18 difference traces	1	21	0

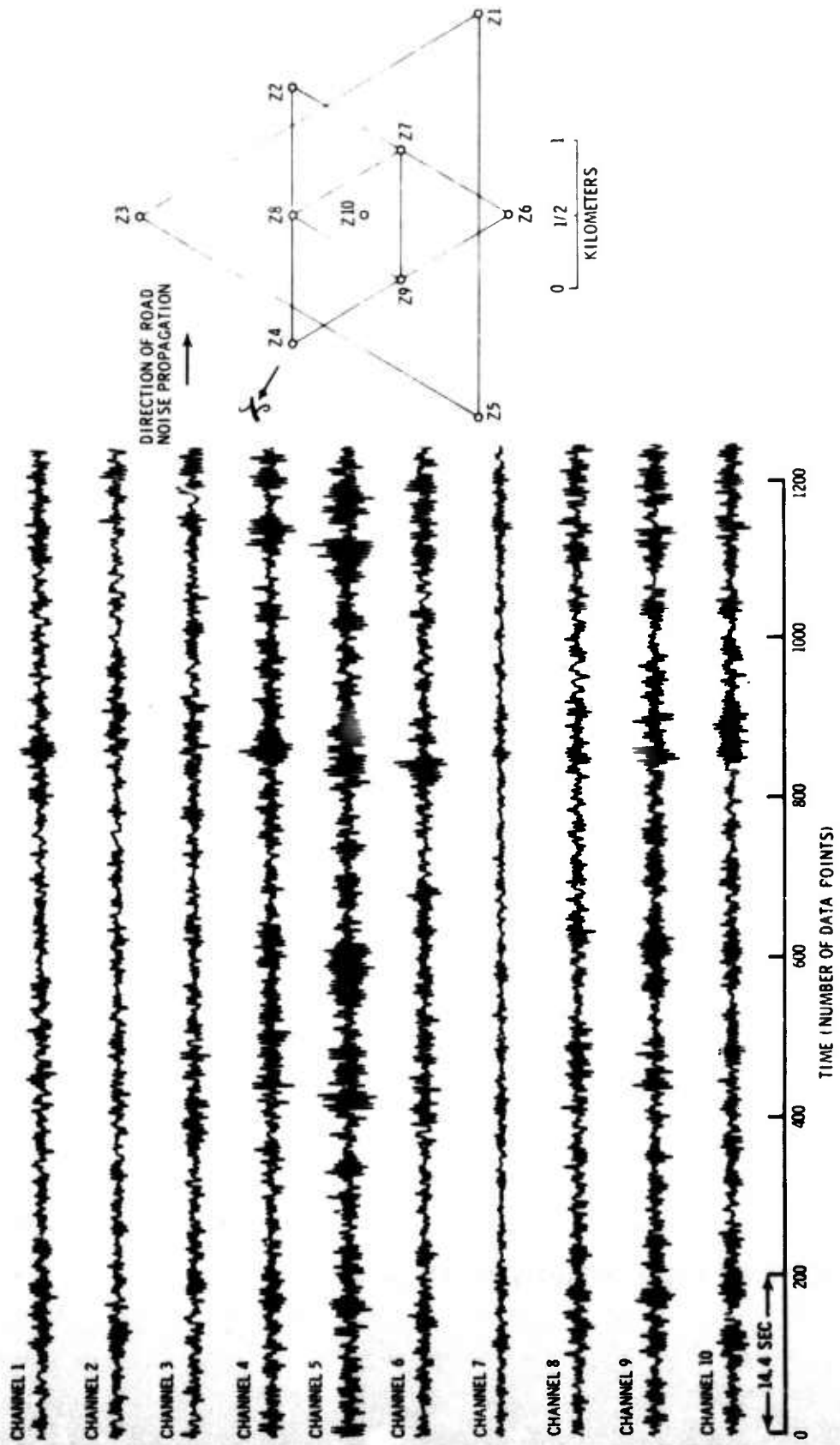


Figure III-1. Prefiltered and Resampled UBO Road Noise and UBO Array Geometry



Prior to any multichannel filtering, the data were prefiltered with an antialiasing, slightly prewhitening filter and resampled to a sample period of 72 msec.

A 27-point Wiener filter with its output point at the center of the filter had been designed previously<sup>1</sup> from these data to predict channel 10 using channels 1 through 9. The mean-square prediction error of the Wiener filter, when applied to the normalized design data, was 0.147.

Two adaptive processing runs, consisting of several passes through the data for each run, were made on this road-noise sample. At the beginning of the first pass of each run, the filter coefficients were set to 0; on successive passes, the coefficients initially were equal to their values at the end of the previous pass. The first run consisted of nine passes where  $k_s$  equaled 0.002 on the first pass and was scaled by two-thirds on each successive pass, ending with a value of 0.000117 after eight passes. For the ninth pass,  $k_s$  equaled 0.00005. In the second run, five passes were made, with  $k_s$  being equal to 0.0005 on the first pass; this was incremented by 0.0005 for each additional pass. Figure III-2 plots as a function of  $k_s$  the mean-square prediction error for each of these passes, excluding the first two in each run which were learning passes.

The fact that the adaptive filter does better than the Wiener filter for intermediate values of  $k_s$  is attributed to the nonstationarity of UBO road noise. Figure III-3 shows mean-square-error over 50-point intervals as a function of location in the data sample. The Wiener and small  $k_s$  adaptive plots are similar, while the plot for the strongly adapting filter appears to be independent of the others. This result supports the hypothesis that UBO road noise is highly nonstationary.

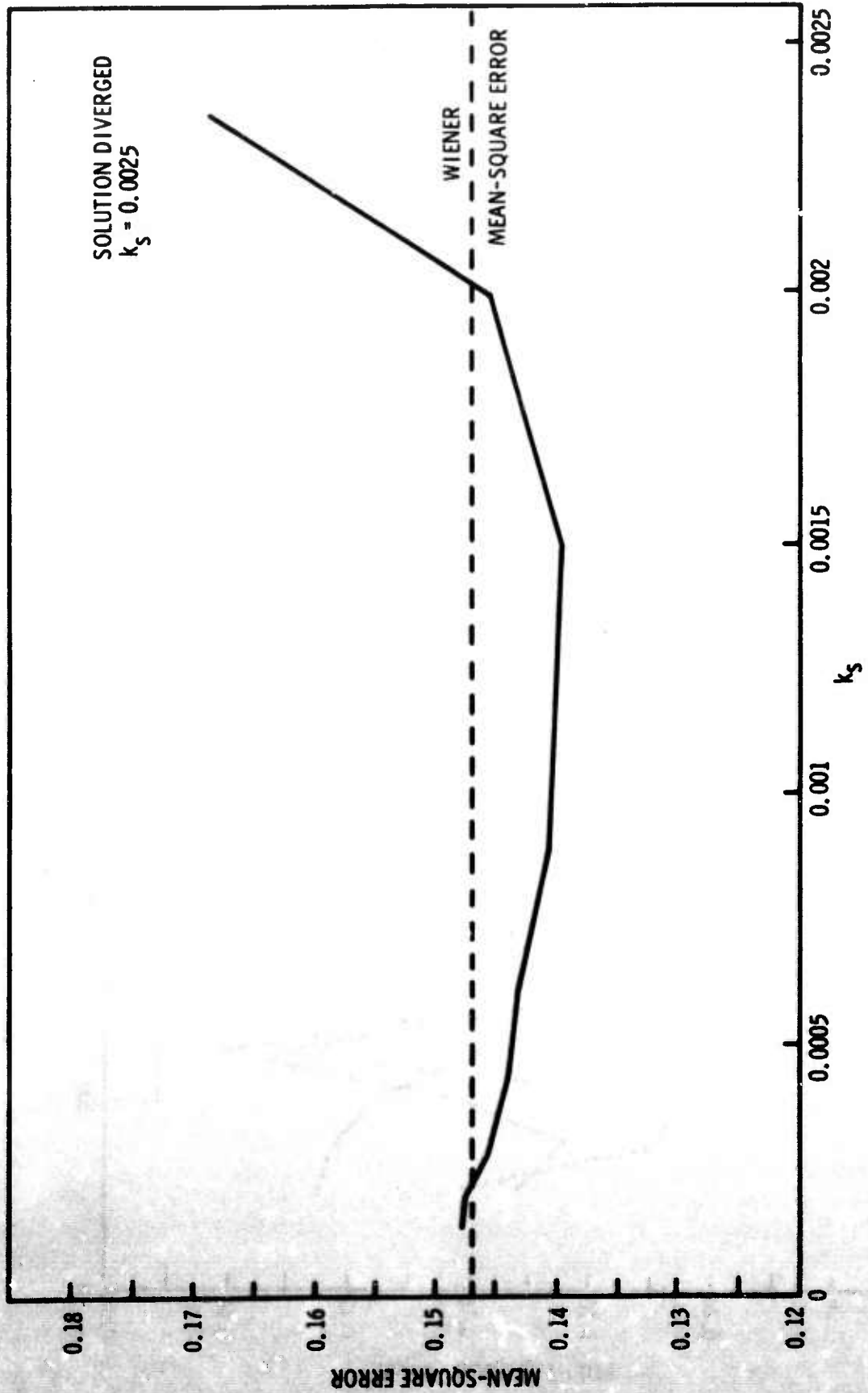


Figure III-2. UBO Road Noise, Mean-Square-Error Vs  $k_s$

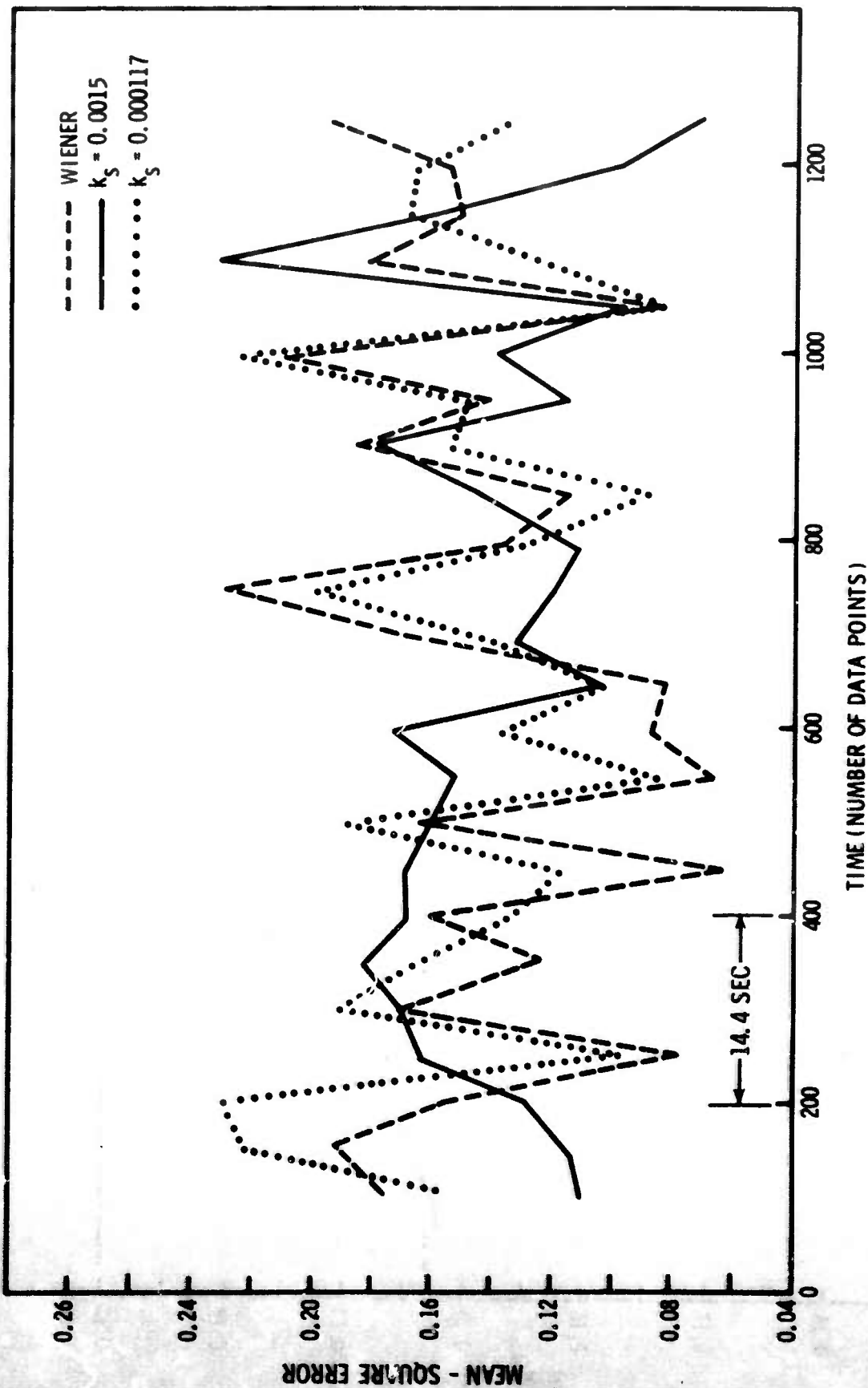


Figure III-3. UBO Road Noise, Mean-Square-Error Vs Time



Figure III-4 shows the energy of the power spectrum of channel 10 to be concentrated around 2.5 cps. The 2.5-cps peak is reduced least by the Wiener filter and is reduced most by the  $k_s = 0.0015$  filter, with the  $k_s = 0.00005$  filter falling between. Additional evidence of the nonstationarity of the data is the dissimilarity between the Wiener and the  $k_s = 0.0015$  error spectra.

Figure III-5 shows channel 10 (the channel being predicted) as well as the prediction and prediction error for the Wiener and small and large  $k_s$  filters.

## 2. UBO Normal Noise

A sample of UBO data, called normal noise because it appears to travel across the array as unattenuated plane waves, is shown in Figure III-6. The UBO normal-noise sample was prefiltered, resampled, normalized, and Wiener-filtered with the same procedures used for the UBO road noise. The normalized mean-square prediction error of the Wiener filter was 0.28.

Three adaptive processing runs were made, one with eight passes and two with one pass with the filter weights being initially set to 0 at the beginning of each run. For the eight passes,  $k_s$  had the values of 0.0015 (learning), 0.0015, 0.001, 0.0005, 0.00025, 0.000125, 0.00005, and 0.002. Values of  $k_s$  for the second and third runs were 0.0025 and 0.003, respectively. Figure III-7 shows the mean-square-error from all runs (except the first learning pass).

The mean-square-error - vs -  $k_s$  curve for these data differs from the corresponding curve for road noise. Mean-square-error increases with increasing  $k_s$  up to approximately  $k_s = 0.001$  and decreases with increasing  $k_s$  from  $k_s = 0.001$  to 0.0025. Mean-square-error increases above  $k_s = 0.0025$  where the algorithm becomes unstable.

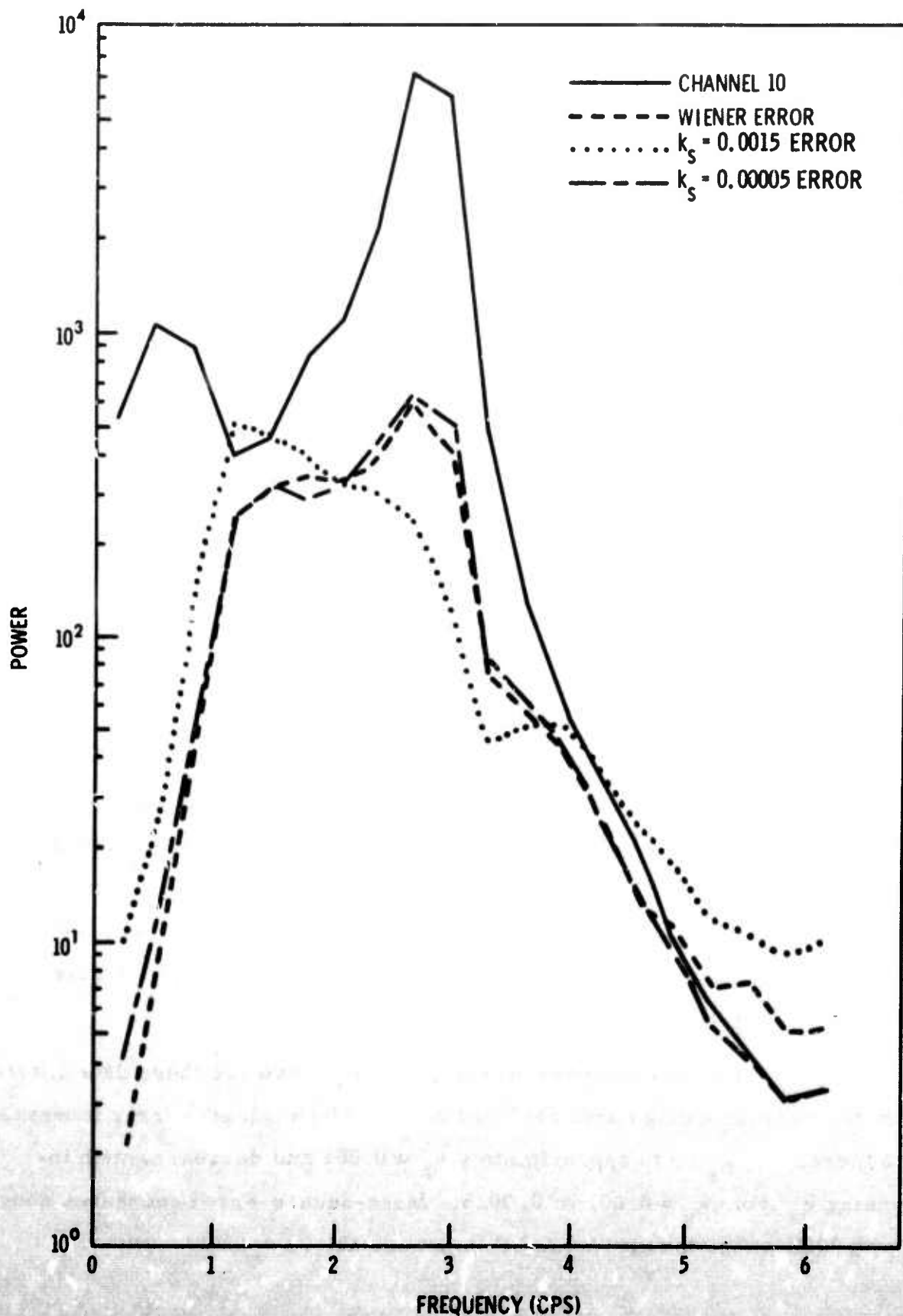


Figure III-4. UBO Road Noise, Power Spectra of Channel 10, Wiener Error, and Adaptive Errors



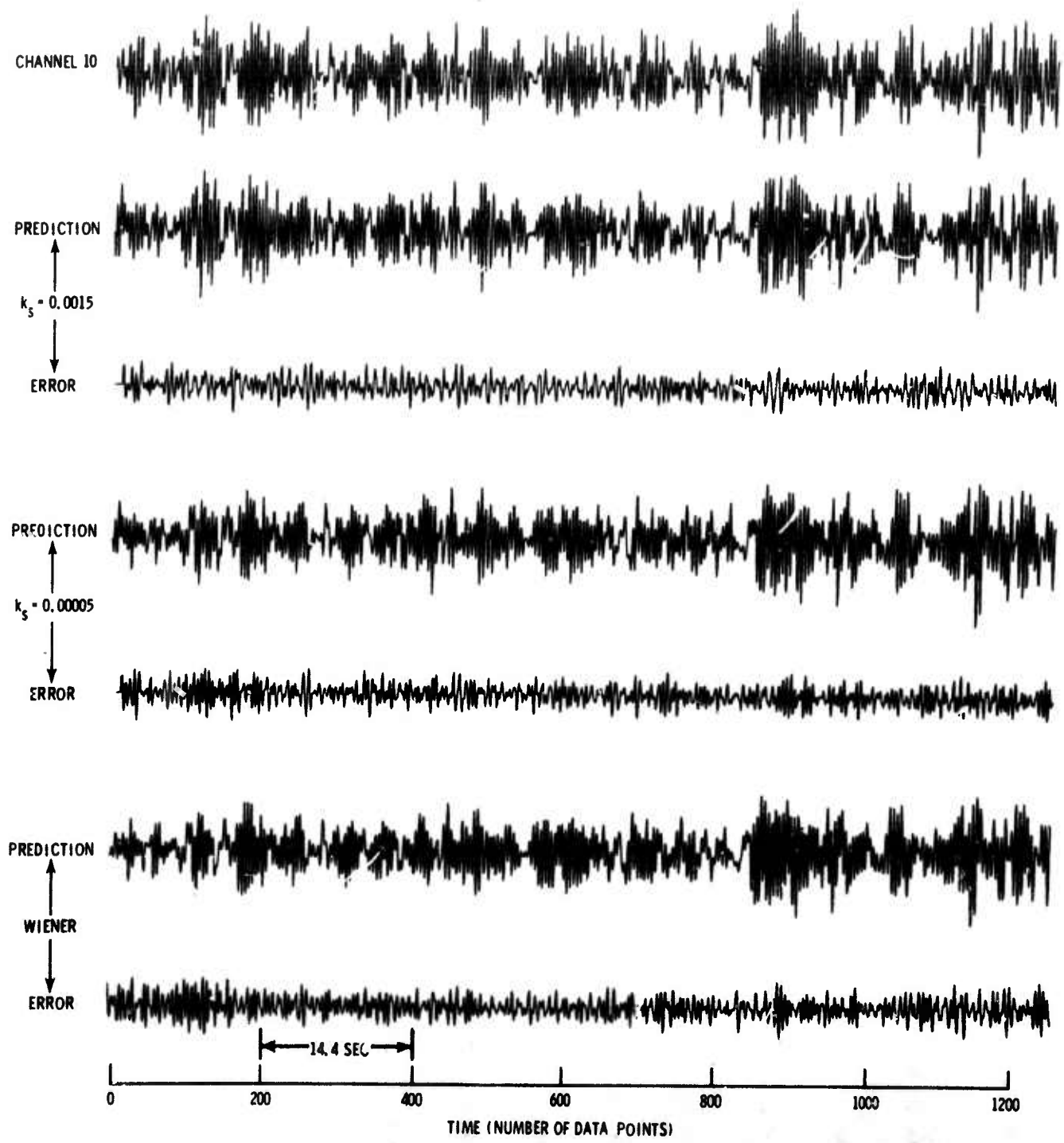


Figure III-5. UBO Road Noise, Wiener and Adaptive Filter Outputs

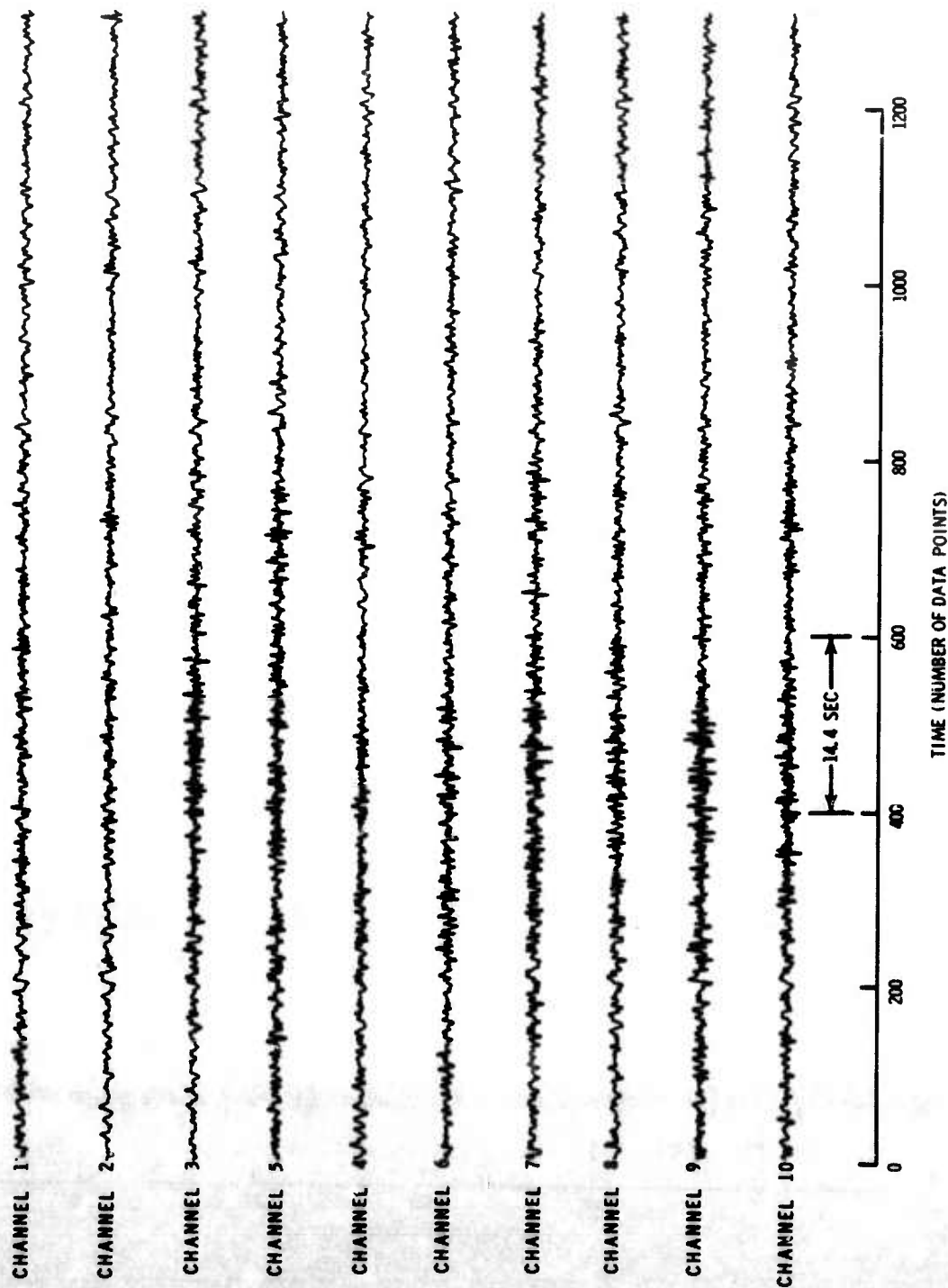


Figure III-6. Prefiltered and Resampled UBO Normal Noise

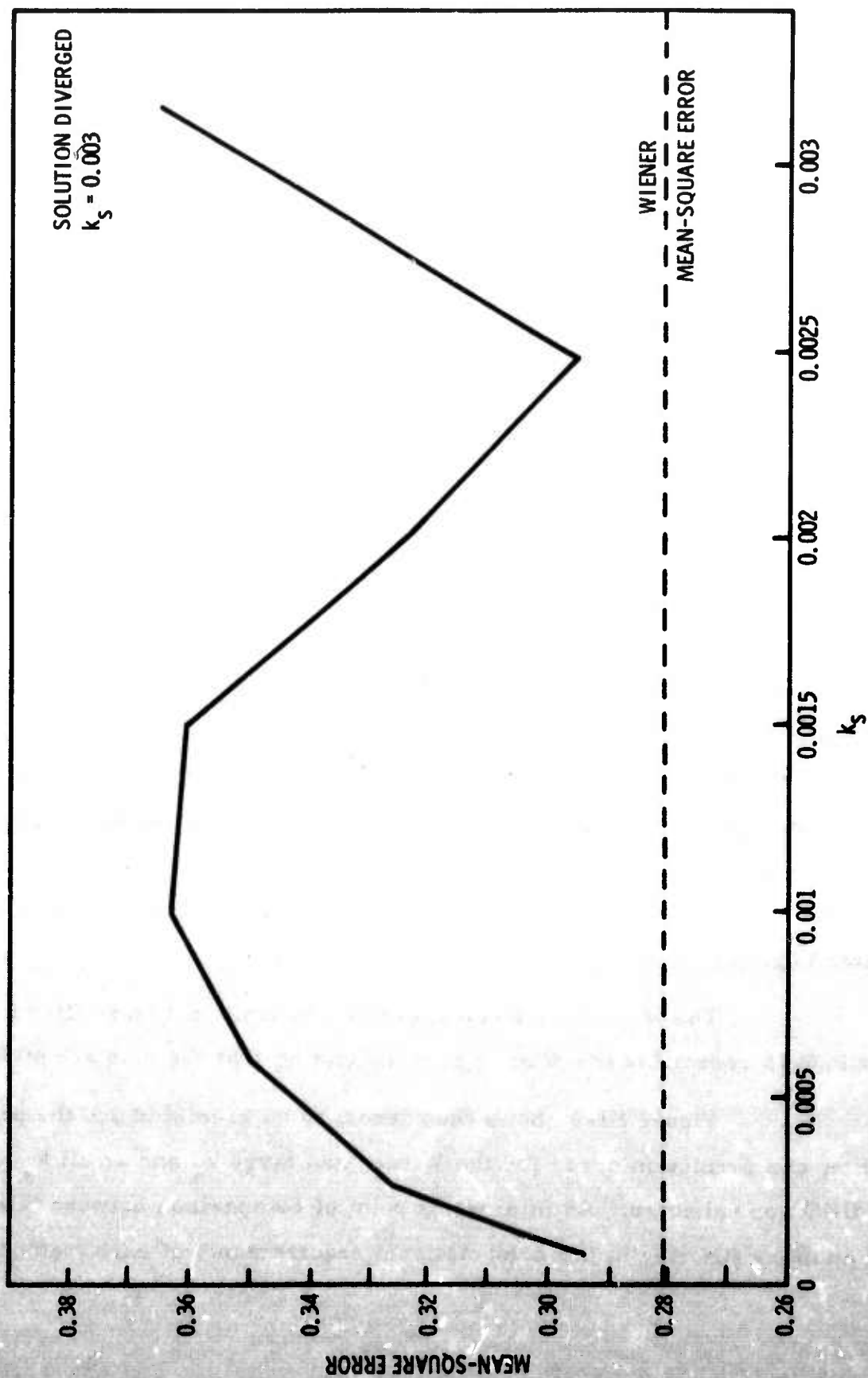


Figure III-7. UBO Normal Noise, Mean-Square-Error Vs  $k_s$



Increasing mean-square-error with increasing  $k_s$  is the expected result for time-stationary data, since a larger  $k_s$  corresponds to a smaller time constant. Thus, the effective length of the data used in designing the filter is decreased, which means statistically that the misdesign and MSE of the filter are increased.

The dip in the MSE at  $k_s = 0.0025$  in Figure III-7 is surprising. One possible explanation for this phenomenon is that the data are time varying, with a time constant which matches the adaptive time constant corresponding to  $k_s = 0.0025$ . This is probably not the correct reason for the dip since a similar effect is seen in other MSE-vs- $k_s$  curves (Figures III-11 and III-16). A more likely explanation is that this decrease in mean-square-error is a false-gain effect caused by the narrow frequency bandwidth of the data. The second interpretation is based on the fact that a data point in a narrowband time series can be well predicted using the recent past of the trace. At first glance, this observation does not appear to apply because only data from channels 1 through 9 are used to predict channel 10. However, the adaptive filter, by means of the error term in the adaptive algorithm, is influenced by the channel 10 data values. Thus, indirectly, the adaptive-filter prediction does use the immediate past of channel 10, with the immediate past being more emphasized for larger values of  $k_s$ . This phenomenon will be discussed further in a later report.

The plot of mean-square-error vs time in Figure III-8 for  $k_s = 0.0015$  resembles the Wiener plot, indicating that the data are stationary.

Figure III-9 shows the channel to be predicted and the prediction and prediction error for the Wiener and large  $k_s$  and small  $k_s$  cases for UBO normal noise. An interesting point of comparison between Wiener and adaptive filtering is the computational requirements of each method.

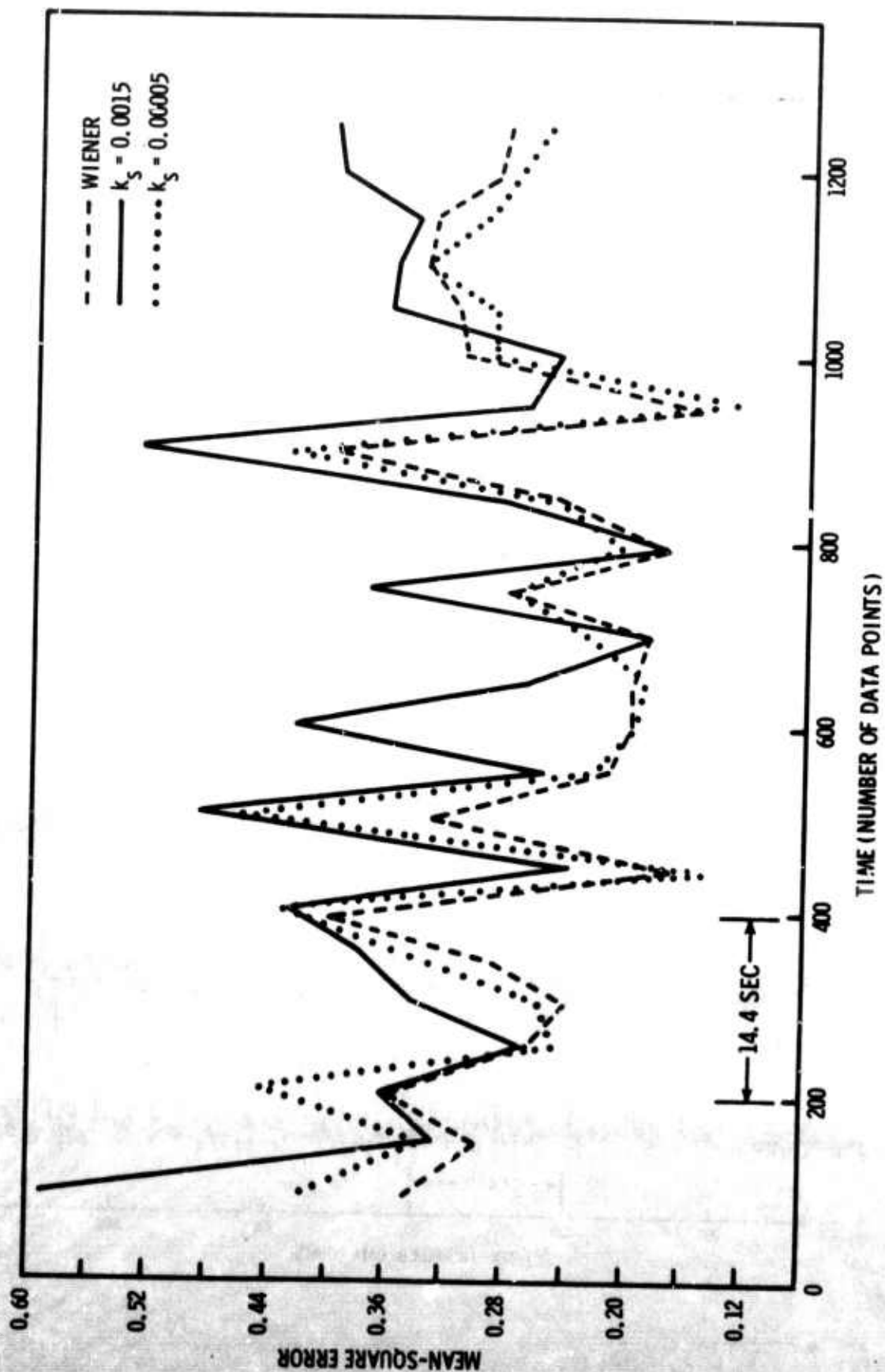


Figure III-8. Normal Noise, Mean-Square-Error  $V_s$  Time

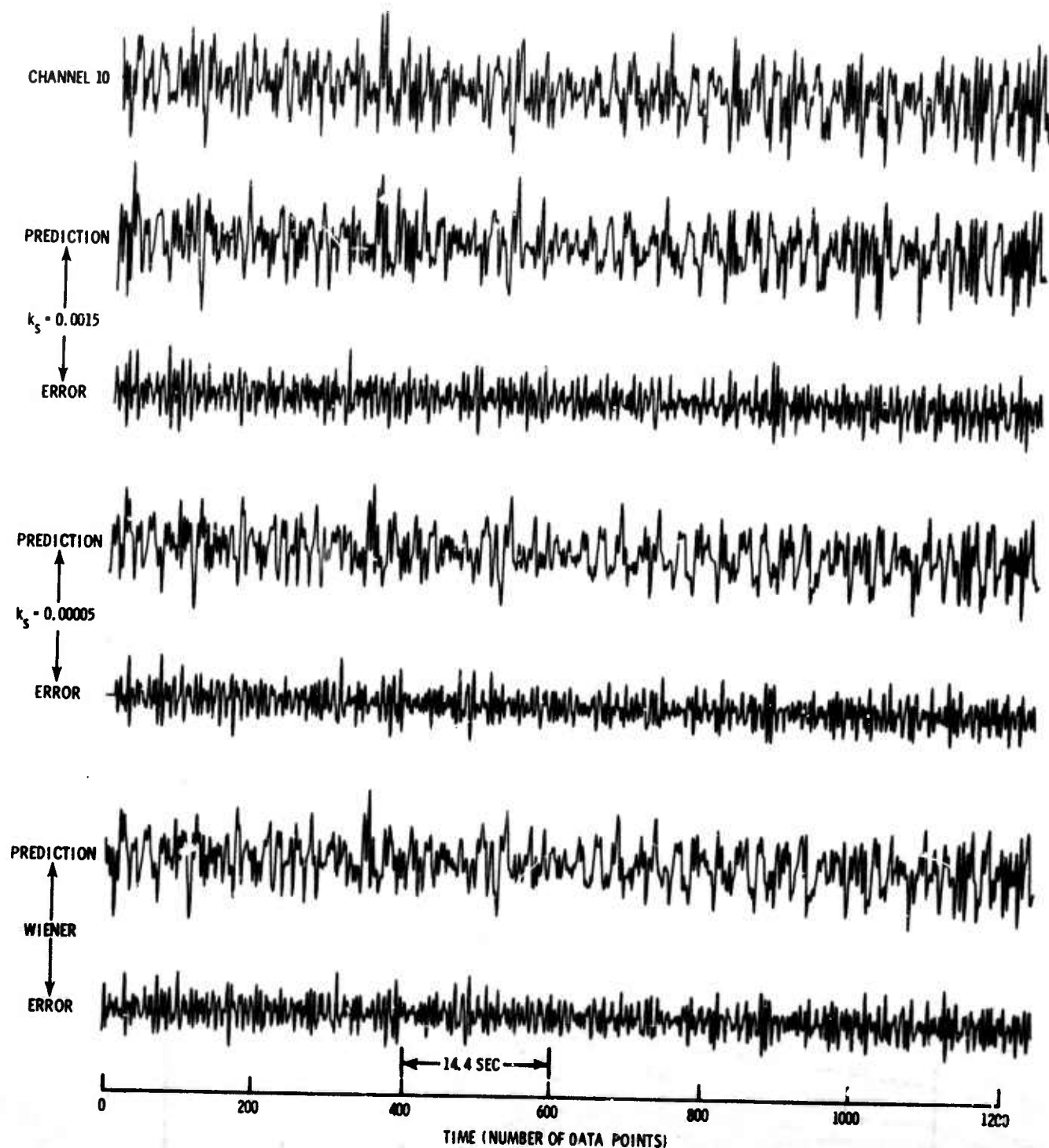


Figure III-9. UBO Normal Noise, Wiener and Adaptive Filter Outputs





On the IBM 7044, the total time to design and apply the Wiener filters to UBO normal noise was 30 min. The procedure involved five separate runs. One run of three adaptive passes through the data would require less than 9 min and would result in approximately the same filters.

### 3. LASA Subarray B1

Another data set used the center seismometer and the first ring of LASA subarray B1. The data shown in Figure III-10 have been antialias-filtered and resampled to a sample rate of 100 msec. Wiener filters, 20-points long, were designed to predict one point ahead on channel 1 based on channels 1 through 7. The resulting normalized mean-square-error was 0.031.

One adaptive filtering run of eight passes was made on these data with  $k_s$  values of 0.0015 (learning), 0.0015, 0.001, 0.0005, 0.00025, 0.000175, 0.0001, 0.00005, and 0.002. The mean-square-error - vs -  $k_s$  curve (Figure III-11) resulting from the adaptive filtering of these data has the same concave-downward shape as seen for UBO normal noise. The plot for  $k_s = 0.001$  (Figure III-12) resembles the  $k_s = 0.00005$  curve enough that the data can be considered time-stationary, although not to the extent of the UBO normal noise. The question of a concave-upward or concave-downward shape for the mean-square-error - vs -  $k_s$  curve apparently involves the time-stationarity of the data.

The power spectrum of channel 1 (Figure III-13) shows no dominant high frequency as is the case for UBO road noise. The similarity in the spectra of the  $k_s = 0.001$  error and the  $k_s = 0.00005$  error is further indication of the stationarity of this data sample.

Figure III-14 shows the Wiener and adaptive filtering results for this LASA data set.

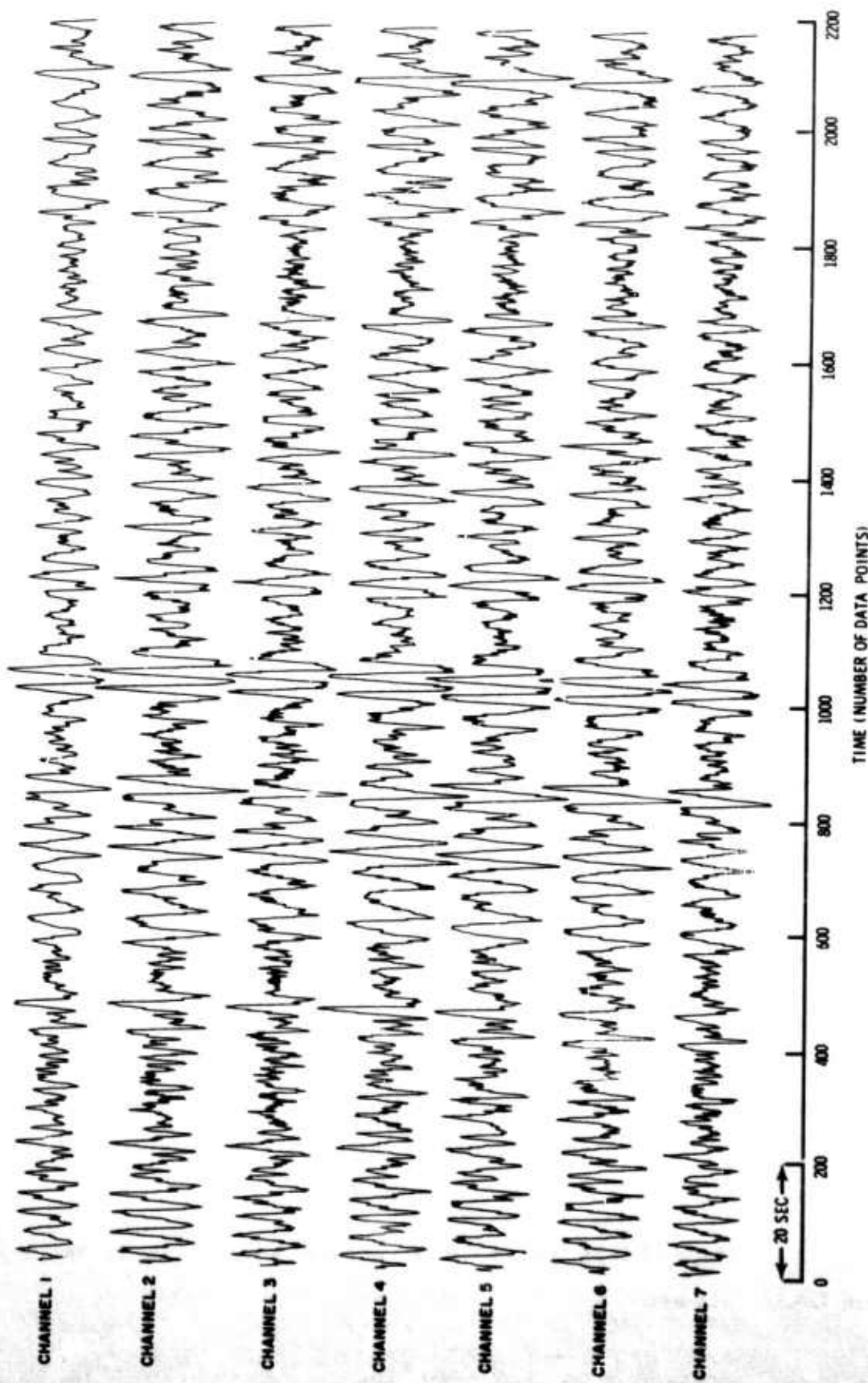


Figure III-10. LASA Subarray B1 Center Seismometer and First Ring Prefiltered and Resampled



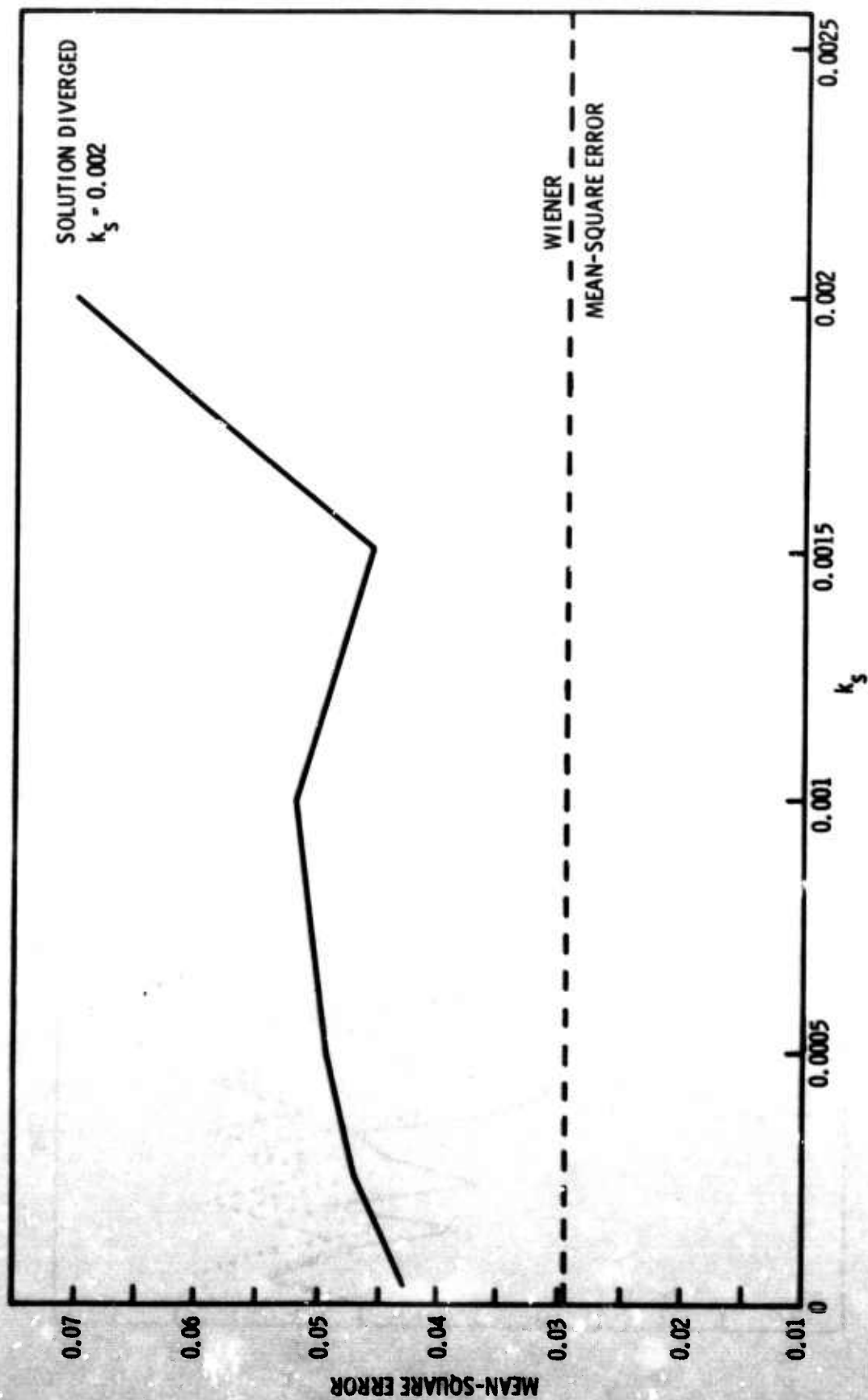


Figure III-11. LASA Subarray B1 Center Seismometer and First Ring, Mean-Square-Error Vs  $k_s$

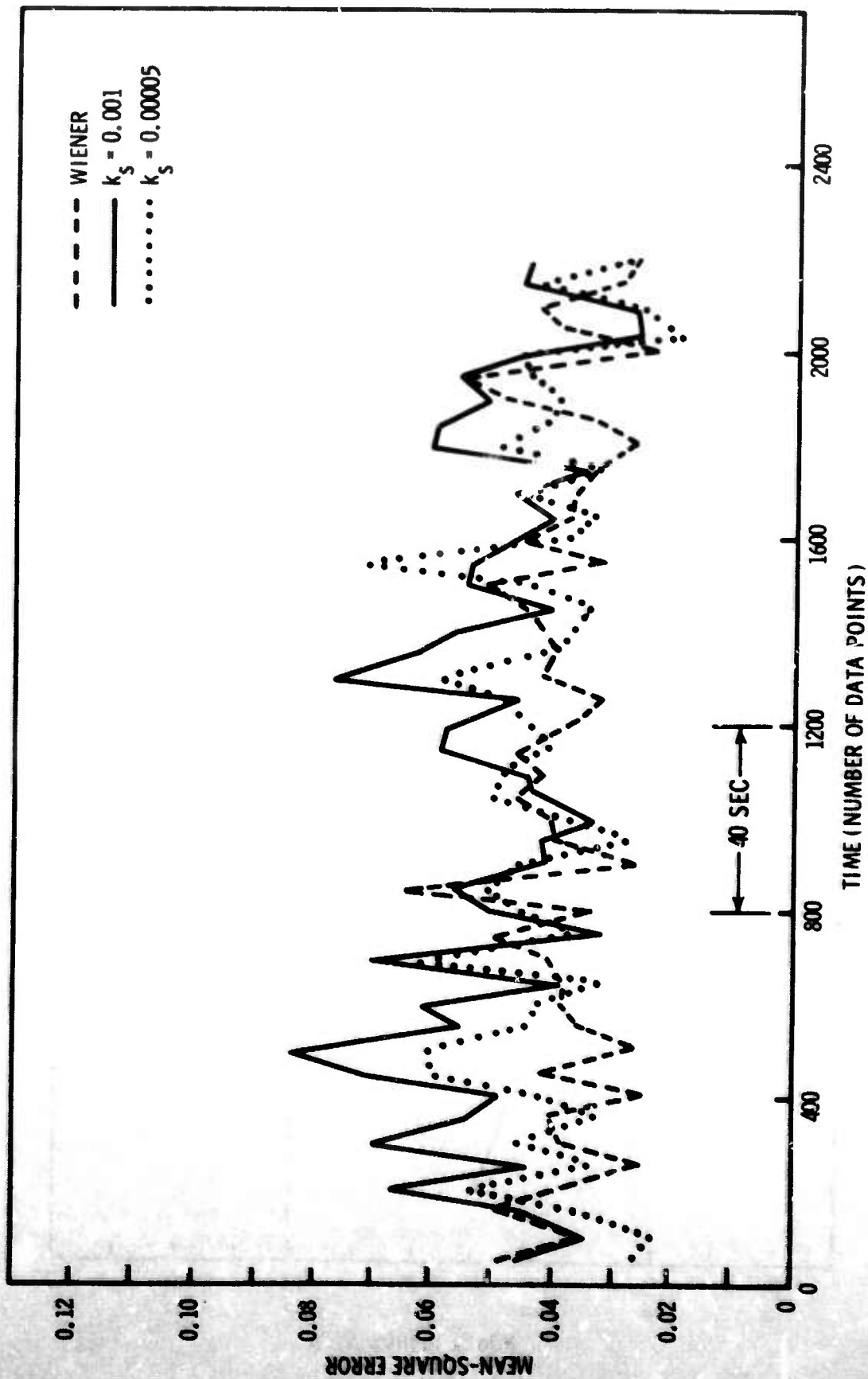


Figure III-12. LASA Subarray B1 Center Seismometer and First Ring, Mean-Square-Error Vs Time

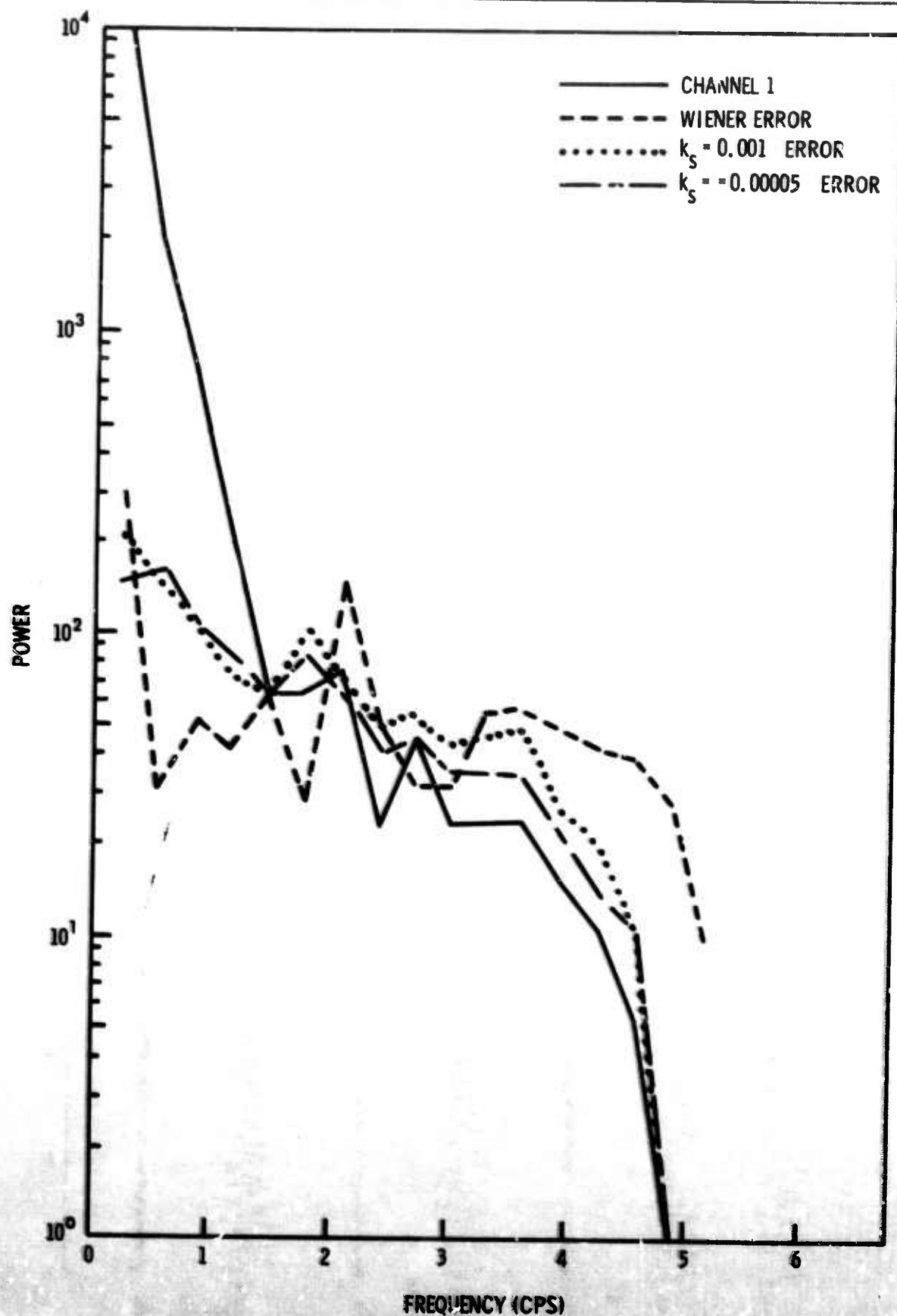


Figure III-13. LASA Subarray B1 Center Seismometer and First Ring — Power Spectra of Channel 1, Wiener Error, and Adaptive Errors

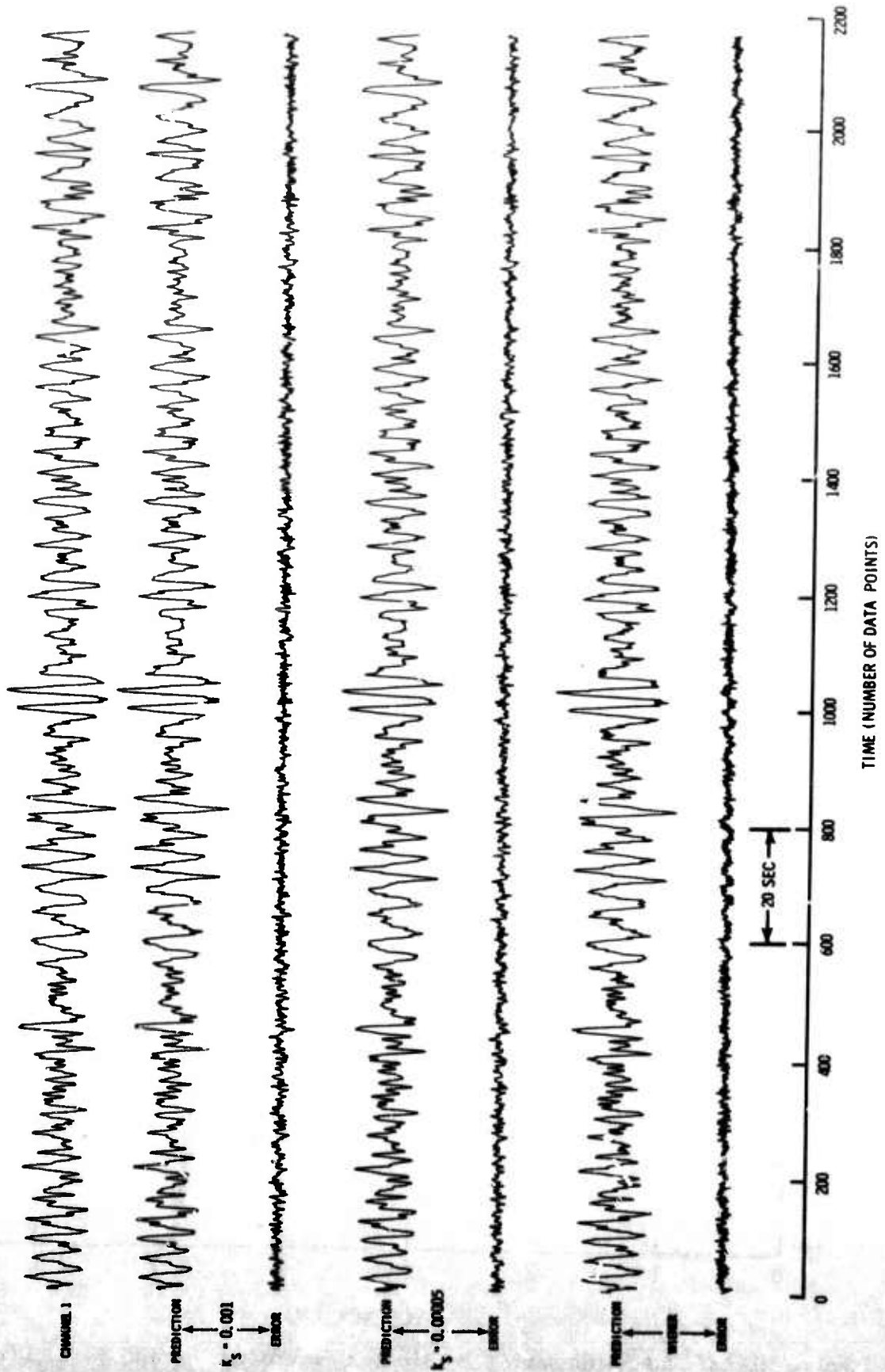


Figure III-14. LASA Subarray B1 Center Seismometer and First Ring, Wiener and Adaptive Filter Outputs



#### 4. Array Data

The 13 channels of array data shown in Figure III-15 have been prewhitened and resampled. A 37-point Wiener filter, with output point at the center, was designed for these data to predict channel 1 from channels 2 through 13. The resulting normalized mean-square-error was 0.16.

Starting with the filter weights set to 0, one adaptive-filtering run having six passes with  $k_s$  values of 0.0005 (learning), 0.0005, 0.00025, 0.000125, 0.00005, and 0.00075 was made on these data. Figure III-16 shows intermediate values of  $k_s$  resulting in errors smaller than the Wiener mean-square-error. In Figure III-17, the dissimilarity between the Wiener and the  $k_s = 0.0005$  plots, especially in the first part of the data, indicates that the data are nontime-stationary. (The behavior of the UBO road noise was the same and was also nontime-stationary.)

Figure III-18 shows the predictions, the prediction error, and the channel to be predicted for the Wiener and large  $k_s$  and small  $k_s$  filters.

#### B. MAXIMUM-LIKELIHOOD FILTERING

To compare adaptive maximum-likelihood filtering with conventional maximum-likelihood filtering, the same basic multichannel data used by SDL in their conventional maximum-likelihood study<sup>2</sup> were used for our adaptive maximum-likelihood work. These data, which came from LASA subarray C1, consisted of 19 of the possible 25 subarray channels, the six seismometers in the inner ring being omitted. A 3250-point, 100-msec sampling-period data segment, which included the signal arrival from an Aleutian Islands event, was the common data. The time traces were prepared by first filtering them with a 0.8- to 2.8-cps bandpass filter, which was thought to be the same as in the SDL study, and then time-shifting them to align the signal.

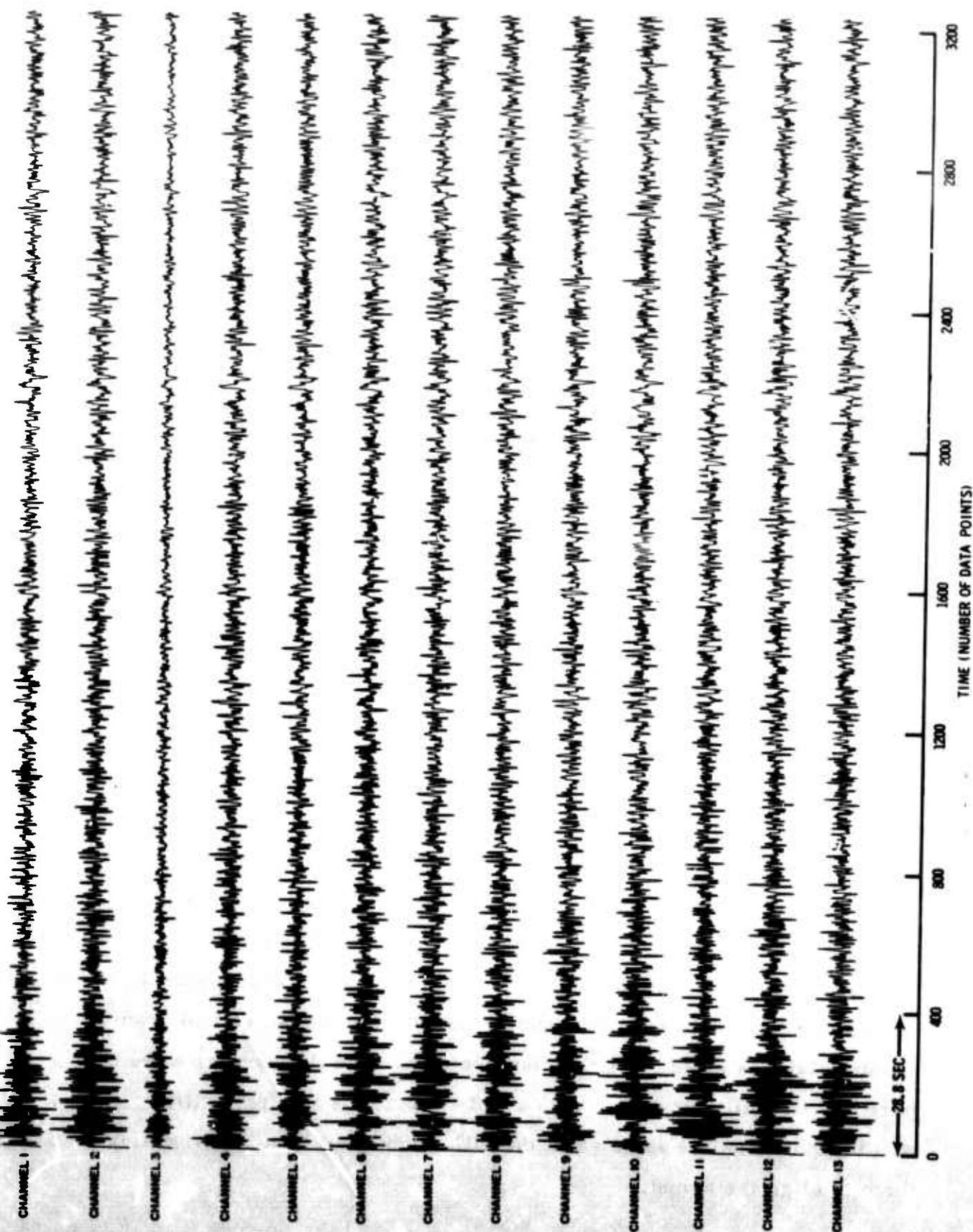


Figure III-15. Prefiltered and Resampled Array Data



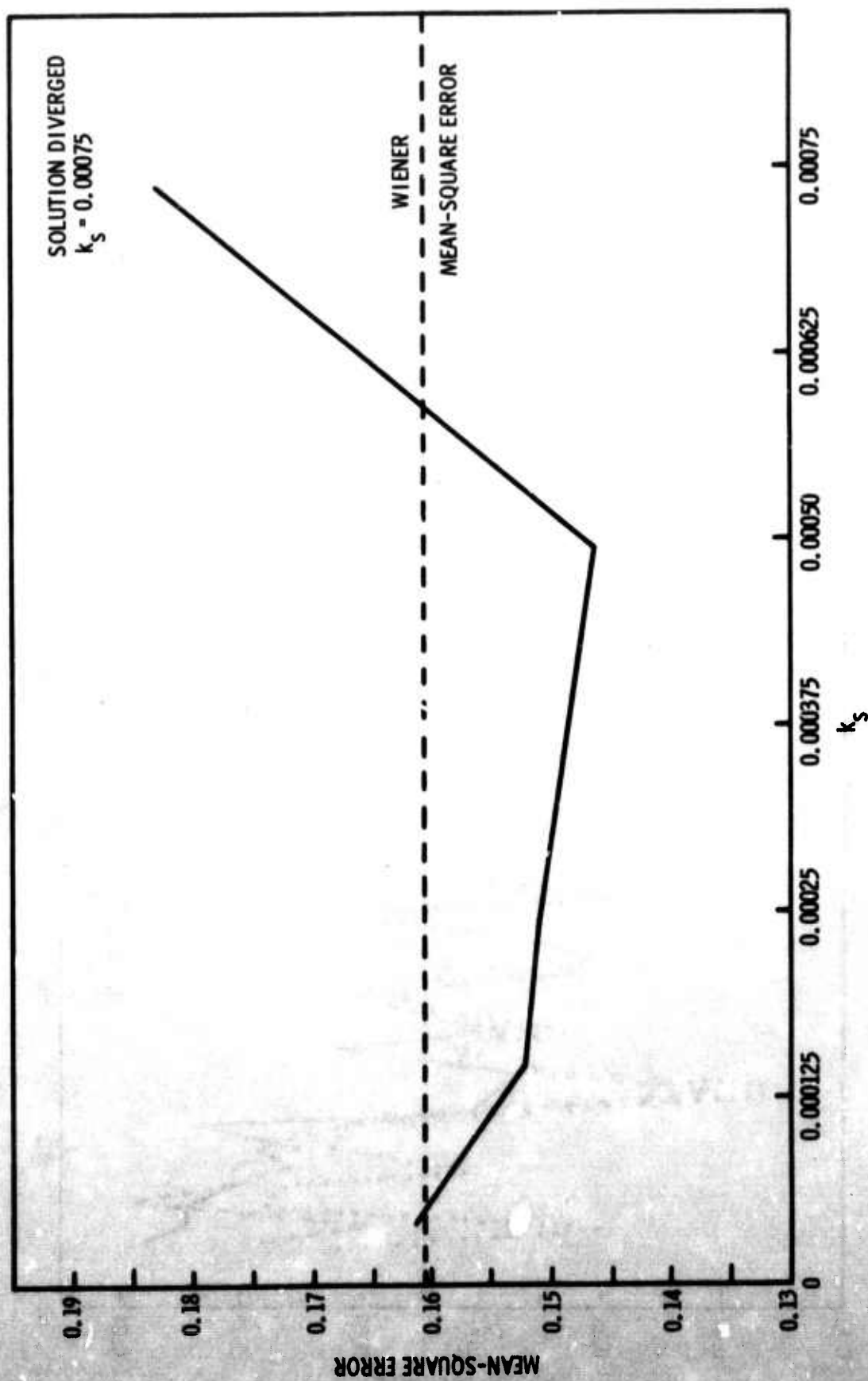


Figure III-16. Array Data, Mean-Square-Error Vs  $k_s$

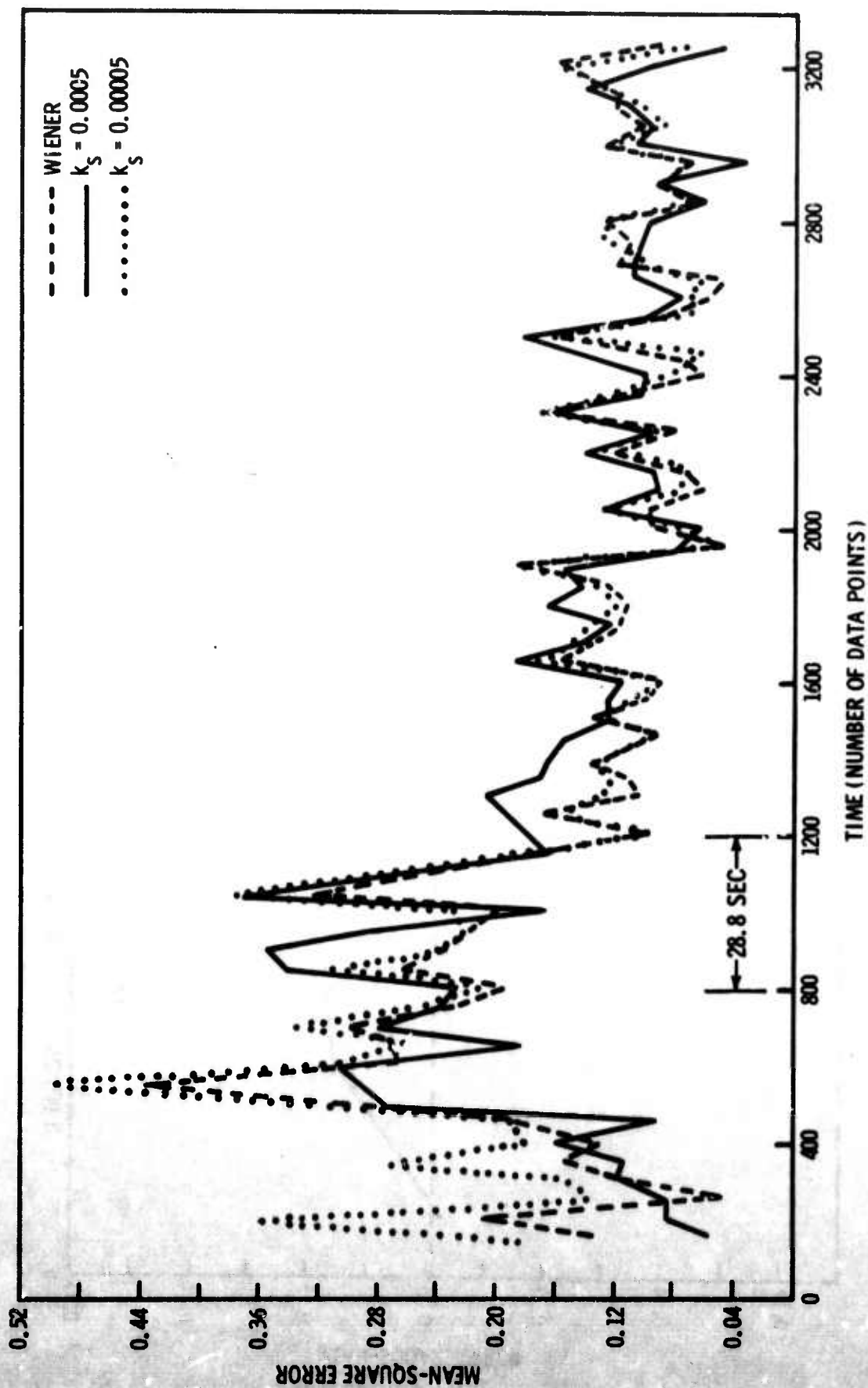


Figure III-17. Array Data, Mean-Square-Error Vs Time



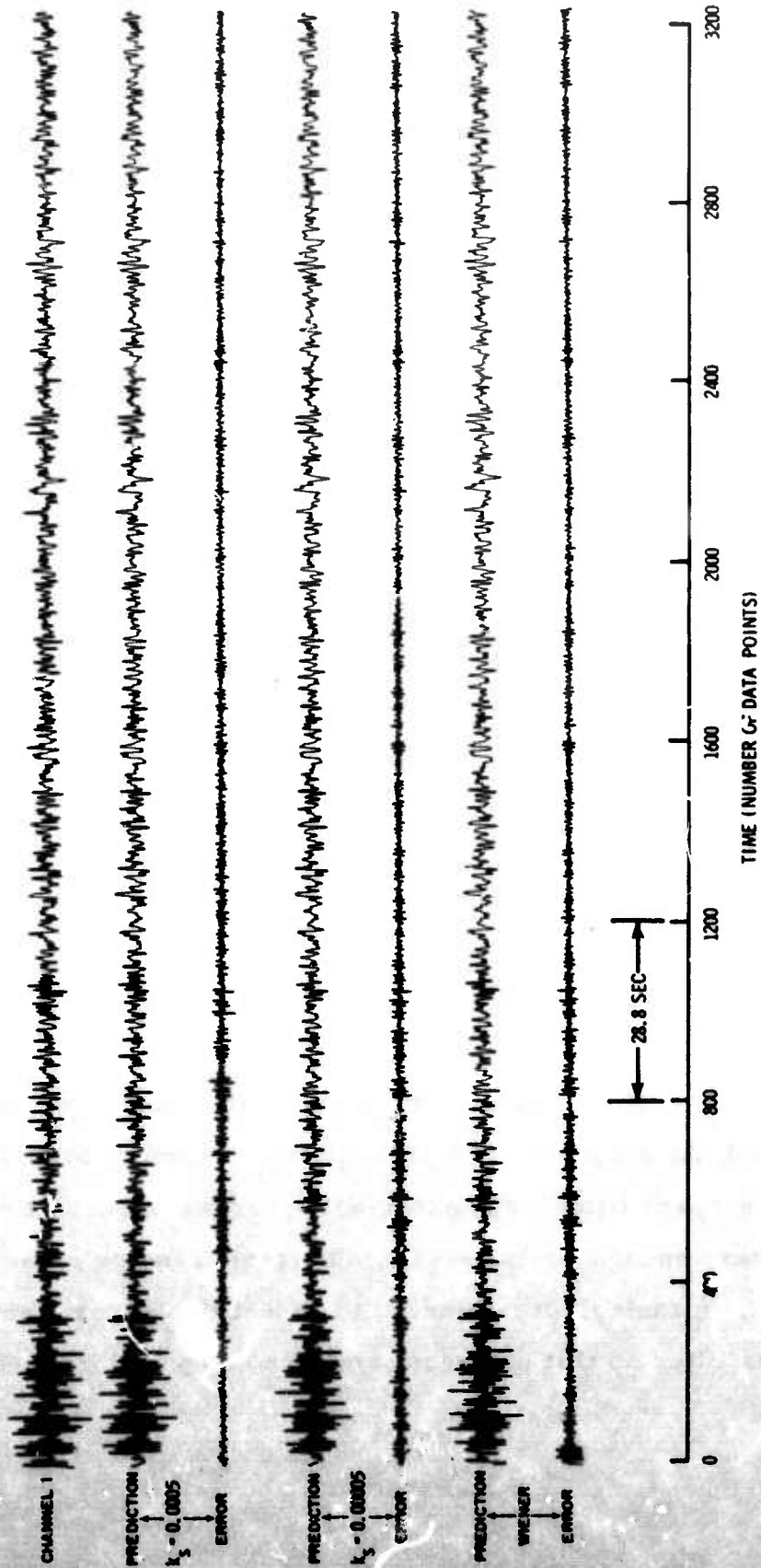


Figure III-18. Array Data, Wiener and Adaptive Filter Outputs



To form a prediction problem, traces 2 through 19 were subtracted from channel 1, yielding 18 difference traces that were normalized and used to predict channel 1, which was also normalized to a variance of 1.

One-sided, 21-point adaptive maximum-likelihood filters, similar to the SDL filters, were designed by two methods. The first, beginning with the filter weights set to 0, included three passes through the data interval from 750 to 2250 points, starting with  $k_s = 0.0005$  for the first pass and using decreasing values of  $k_s$  (0.00025, 0.00005) for each successive pass. At the end of the third pass, the filters were fixed and the entire data sample was filtered with these fixed filters. The SDL conventionally designed maximum-likelihood filter used the same 750- to 2250-point filtering interval. The second method began with filter weights of 0, used a  $k_s$  of 0.00005, and let the filters operate on-line (i.e., adapt and filter) for one pass through the data.

Figure III-19 shows the outputs of a phased sum, the conventional maximum-likelihood filter, and the two types of adaptive maximum-likelihood filters. As can be seen, the adaptively designed fixed filter is essentially equivalent in performance to that of the SDL-designed filter. The on-line filter, which had been adapting for 1725 points at the beginning of the shown trace, is about 3-db poorer than the off-line filters.

It was planned to have a quantitative comparison of the SDL filter with the adaptively designed filter. However, the frequency response of our bandpass filter was appreciably narrower than that of the SDL bandpass filter, enough so that measured signal-to-noise ratio improvements have little meaning. It is planned to repeat this experiment using the SDL bandpass filter so that our results can be compared in a more precise manner.

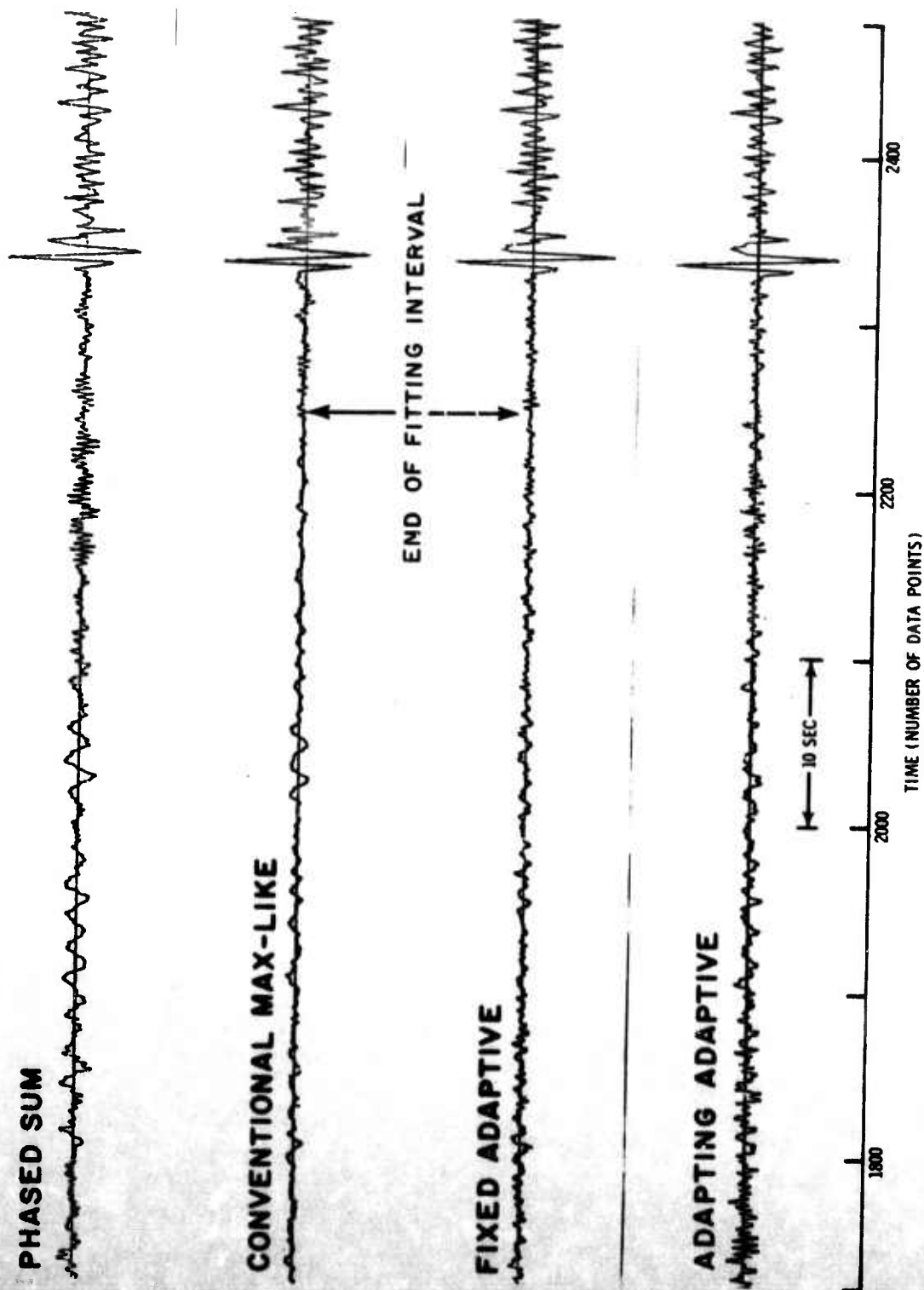


Figure III-19. Maximum-Likelihood Filter Outputs



## SECTION IV

### CONCLUSIONS AND RECOMMENDATIONS

From the theory of adaptive filtering, adaptive prediction filtering results would be expected to show several things. The adaptive filter should approach the Wiener filter as  $k_s$  approaches 0. This convergence, which was not explicitly searched for, seems to be true experimentally.

Another expected result is that the adaptive mean-square-error may be less than the Wiener mean-square-error if the data are time-varying but should always be greater if the data are stationary. The excess mean-square-error for stationary data can be shown to result from random oscillations of the filter coefficients about their optimum values.<sup>3</sup> Smaller adaptive mean-square-errors for nonstationary data are produced by the ability of the filters to track the changing minimum of the quadratic error-squared surface. These theoretical expectations seem to be verified in general by our experimental results. The exception is the interesting phenomenon of the dip in mean-square-error for large values of  $k_s$  (just before the algorithm becomes unstable). This MSE decrease, which is thought to be false gain caused by the narrow frequency bandwidth of the data, is a subject for future study. The final expected theoretical result is that, as  $k_s$  increases, a point is reached where the algorithm becomes unstable. A study of the parameters controlling the stability of the algorithm is being made.



The following summarizes our conclusions and recommendations.

- Results of this study indicate that, in the limit as  $k_s$  approaches 0, the resulting adaptive filter approaches the Wiener filter; therefore, the adaptive processing scheme could be of value as an economical means of Wiener filter design
- As data statistics change, the optimum value of  $k_s$  changes; therefore, the investigation of methods of varying  $k_s$  with changing data statistics is recommended
- Some data samples, when filtered adaptively, result in concave-downward mean-square-error-vs- $k_s$  curves while other data samples result in a concave-upward curve; preliminary results given in this report indicate that the data characteristic which determines the shape of this curve is related to the time-stationarity of the data
- Adaptive maximum-likelihood filtering results indicate that this type of filtering can be done with much less time and expense than required by conventional means
- The inclusion of methods of extending the adaptive filtering concepts to the problem of signal extraction based on a theoretical signal model is recommended for any future study
- Only one prewhitened sample is included in the data processed here; the other three samples will be prewhitened and adaptively filtered by the same procedure used on the raw data in this report in order to determine the effects of prewhitening on adaptive filtering, and a later report will present these results



---

SECTION V  
REFERENCES

1. Texas Instruments Incorporated, 1966: Uinta Basin Observatory Multichannel Filter Design and Evaluation, Contract AF 33(657)-12747, 20 Sep.
2. Teledyne, Inc., 1966: Two Examples of Maximum-Likelihood Filtering of LASA Seismograms, Contract AF 33(657)-15919, 8 Jun.
3. Stanford Electronics Laboratories, 1966: Adaptive Filters I: Fundamentals, Tech. Rpt. No. 6764-6, Contract DA-01-021 AMC-90015(Y), Dec.

UNCLASSIFIED

Security Classification

## DOCUMENT CONTROL DATA - R&amp;D

(Security classification of title, body of abstract and indexing annotation must be entered when the overall report is classified)

## 1. ORIGINATING ACTIVITY (Corporate author)

Texas Instruments Incorporated  
Science Services Division  
P.O. Box 5621, Dallas, Texas 75222

## 2a. REPORT SECURITY CLASSIFICATION

Unclassified

## 2b. GROUP

---

## 3. REPORT TITLE

ADAPTIVE FILTERING OF SEISMIC ARRAY DATA  
ADVANCED ARRAY RESEARCH Special Report No. 1

## 4. DESCRIPTIVE NOTES (Type of report and inclusive dates)

Special

## 5. AUTHOR(S) (Last name, first name, initial)

Burg, John P.

Holyer, Ronald J.

Booker, Aaron H.

## 6. REPORT DATE

## 7a. TOTAL NO. OF PAGES

44

## 7b. NO. OF REFS

3

## 8a. CONTRACT OR GRANT NO.

F33657-67-C-0708-P001

## b. PROJECT NO.

VELA T/7701

d.

## 9a. ORIGINATOR'S REPORT NUMBER(S)

---

## 9b. OTHER REPORT NO(S) (Any other numbers that may be assigned this report)

---

## 10. AVAILABILITY/LIMITATION NOTICES

This document is subject to special export controls and each transmittal to foreign governments or foreign nationals may be made only with prior approval of Chief, AFTAC

## 11. SUPPLEMENTARY NOTES

ARPA Order No. 624

ARPA Program Code No. 7F10

## 12. SPONSORING MILITARY ACTIVITY

Advanced Research Projects Agency

Department of Defense

The Pentagon, Washington, D.C., 20301

## 13. ABSTRACT

Adaptive multichannel prediction filtering has been completed on four data samples, and adaptive maximum-likelihood signal extraction has been done on one sample. Comparison of adaptive results with those obtained from processing the same data with stationary filters (nonchanging filters designed from correlation-function estimates) shows that the adaptive filters approach the stationary filters as  $k_s$  (the rate-of-convergence parameter in the adaptive algorithm) approaches 0. For larger values of  $k_s$ , adaptive prediction-error filtering does better than stationary filters on non-time-stationary data, but stationary filters are better on data samples which appear to be time-uniform. The performance of an adaptively designed maximum-likelihood filter was shown to be essentially equivalent to that of a maximum-likelihood filter which was conventionally designed from correlation-function estimates.

DD FORM 1 JAN 64 1473

UNCLASSIFIED

Security Classification



KEY WORDS	LINK A		LINK B		LINK C	
	ROLE	WT	ROLE	WT	ROLE	WT
Advanced Array Research Adaptive Multichannel Prediction Filtering Adaptive Maximum-Likelihood Signal Extraction						

## INSTRUCTIONS

**ORIGINATING ACTIVITY:** Enter the name and address of the contractor, subcontractor, grantee, Department of Defense activity or other organization (*corporate author*) issuing the report.

**REPORT SECURITY CLASSIFICATION:** Enter the overall security classification of the report. Indicate whether "Restricted Data" is included. Marking is to be in accordance with appropriate security regulations.

**GROUP:** Automatic downgrading is specified in DoD Directive 5200.10 and Armed Forces Industrial Manual. Enter the group number. Also, when applicable, show that optional markings have been used for Group 3 and Group 4 as authorized.

**REPORT TITLE:** Enter the complete report title in all capital letters. Titles in all cases should be unclassified. A meaningful title cannot be selected without classification. Show title classification in all capitals in parenthesis immediately following the title.

**DESCRIPTIVE NOTES:** If appropriate, enter the type of report, e.g., interim, progress, summary, annual, or final. Give the inclusive dates when a specific reporting period is covered.

**AUTHOR(S):** Enter the name(s) of author(s) as shown on the report. Enter last name, first name, middle initial. If military, show rank and branch of service. The name of the principal author is an absolute minimum requirement.

**REPORT DATE:** Enter the date of the report as day, month, year, or month, year. If more than one date appears on the report, use date of publication.

**TOTAL NUMBER OF PAGES:** The total page count should follow normal pagination procedures, i.e., enter the number of pages containing information.

**NUMBER OF REFERENCES:** Enter the total number of references cited in the report.

**CONTRACT OR GRANT NUMBER:** If appropriate, enter the applicable number of the contract or grant under which the report was written.

**7c, & 8d. PROJECT NUMBER:** Enter the appropriate military department identification, such as project number, project number, system numbers, task number, etc.

**ORIGINATOR'S REPORT NUMBER(S):** Enter the official report number by which the document will be identified and controlled by the originating activity. This number must be unique to this report.

**OTHER REPORT NUMBER(S):** If the report has been assigned any other report number(s) (*either by the originator or by the sponsor*), also enter this number(s).

**AVAILABILITY/LIMITATION NOTICES:** Enter any limitations on further dissemination of this report, other than those

imposed by security classification, using standard statements such as:

- (1) "Qualified requesters may obtain copies of this report from DDC."
- (2) "Foreign announcement and dissemination of this report by DDC is not authorized."
- (3) "U. S. Government agencies may obtain copies of this report directly from DDC. Other qualified DDC users shall request through \_\_\_\_\_."
- (4) "U. S. military agencies may obtain copies of this report directly from DDC. Other qualified users shall request through \_\_\_\_\_."
- (5) "All distribution of this report is controlled. Qualified DDC users shall request through \_\_\_\_\_."

If the report has been furnished to the Office of Technical Services, Department of Commerce, for sale to the public, indicate this fact and enter the price, if known.

**11. SUPPLEMENTARY NOTES:** Use for additional explanatory notes.

**12. SPONSORING MILITARY ACTIVITY:** Enter the name of the departmental project office or laboratory sponsoring (paying for) the research and development. Include address.

**13. ABSTRACT:** Enter an abstract giving a brief and factual summary of the document indicative of the report, even though it may also appear elsewhere in the body of the technical report. If additional space is required, a continuation sheet shall be attached.

It is highly desirable that the abstract of classified reports be unclassified. Each paragraph of the abstract shall end with an indication of the military security classification of the information in the paragraph, represented as (TS), (S), (C), or (U).

There is no limitation on the length of the abstract. However, the suggested length is from 150 to 225 words.

**14. KEY WORDS:** Key words are technically meaningful terms or short phrases that characterize a report and may be used as index entries for cataloging the report. Key words must be selected so that no security classification is required. Identifiers, such as equipment model designation, trade name, military project code name, geographic location, may be used as key words but will be followed by an indication of technical context. The assignment of links, rules, and weights is optional.